Vertex-Based Corticometry: Applications to Normal and Pathological Human Brain Development

A Proposal for a Ph.D. Thesis in Neuroscience

By: Yasser Ad-Dab'bagh, M.D., F.R.C.P.(C)

Department of Neurology and Neurosurgery
Department of Psychiatry

17th November, 2003

Contents

Abstract

Cytoarchitectonic variations in different regions of the human cerebral cortex have been shown to result in varying thickness of the cortex. Histological investigations have shown that individual brains of normal subjects differ significantly in sizes and locations of cytoarchitectural areas. On top of this normal variation, pathological conditions may be associated with significant differences in cytoarchitectural organizations in some or most brain regions, depending on the pathology. Studies on post-mortum brains have documented some of these differences in many developmental and degenerative neuropsychiatric disorders. Some attempts have been made to correlate cytoarchitecture with reported behavioral measures and neuropsychiatric diagnoses. Recently, methods for measuring cortical thickness *in vivo* via modern neuro-imaging technology have evolved and may potentially be applied to population studies of the trajectories of global and regional cortical development, and the impact on those trajectories of environmental variables and neuropsychiatric pathology. This thesis proposal aims to establish that a method for measuring cortical thickness in vivo developed at the Montreal Neurological Institute can be applied for such studies.

The proposed project will focus on four areas of investigation: (1) Clinically informed contributions to various methodological components of the process of generating parametric maps of cortical thickness for pediatric samples; (2) The study of normal regional and global growth trajectories of cortical thickness during childhood; (3) The examination of the impact of exposure to nicotine *in utero* on cortical thickness maps of adolescents, as an example of the interaction of cortical development with environmental variables; and (4) The comparison of cortical thickness maps of subjects with the developmental disorder schizophrenia with equivalent maps derived from normal controls. The last area of investigation will involve an examination of the longitudinal impact of the diagnosis on cortical thickness maps in childhood-onset schizophrenia and in adults experiencing their first episode of the illness, as well as an attempt to correlate clinically relevant behavioral observations with these cortical thickness maps. It may also involve a comparison of schizophrenia with other developmental disorders, to illustrate the presence of pathology-specific growth trajectories of cortical thickness. The scientific implications of this form of research range from the establishment of a neural correlate to many developmental neuropsychiatric disorders, to an understanding of the impact of the environment on brain development. Basic science applications of these neuro-anatomical correlates may include establishing animal models for disorders that manifest only with mental dysfunction. Clinical applications may include the examination of the impact of therapeutic interventions on the development of the brain as well as on pathological growth trajectories.

With its potential for numerous publications in peer-reviewed journals, the proposed project is hoped to meet the scientific requirements for a Ph.D. in Neuroscience.

1 Neurobiology of the Cerebral Cortex and its Thickness

1.1 The Structure and Function of the Cerebral Cortex

Among the earliest references to the variable structure of the human cerebral cortex were those of Generi in 1776[4] and Betz in 1874[5], both noting the existence in some regions of the cortex of structures unique to those regions. When Meynert reported regional differences in both cellular structure and cortical laminae in 1867[6], he laid the foundations upon which the work of Brodmann was based at the turn of the twentieth century[7, 8, 9]. Brodmann mapped the cerebral cortex of a single human brain into 52 regions (45 plus regions 7 gaps) of distinctive cytoarchitectonic structure[8], and reported his measurements of cortical laminar thickness which varied based on cell type. Since the work of Brodmann, scientists have continued to elaborate on the cytoarchitecture of the cerebral cortex[11, 12, 13, 14, 15], describing the neocortex as consisting of six laminae, each further subdivided into intermediate laminae based on the varying architectonic characteristics of the defining laminar components.

The thickness of the neocortex is almost always found to be between 2 and 4 mm in histological studies[16]. The thickness of the individual laminae, however, varies depending upon the region of the cerebral cortex. For example, in the frontal lobe, lamina III (the external pyramidal layer) becomes progressively thinner toward the frontal pole, whereas lamina IV (the internal granular layer) becomes thicker toward the frontal pole and nearly nonexistent in the precentral gyrus[17, 16]. These differences are thought to reflect functional differentiation related to the neural networks associated with each region. For example, lamina IV is very prominent in the primary visual cortex, and is thought to be the main target of sensory information arriving from the thalamus (the lateral geniculate nucleus)[16]. In contrast, the precentral gyrus (the primary motor cortex) receives little sensory information directly from the thalamus, which may explain the relative absence of lamina IV[16]. In addition to regional variability, recent cytoarchitectural research documents significant variability in sizes and exact locations of cytoarchitectural areas between individual brains, and between hemispheres of the same brain[13, 14, 15, 18], with greater variability in the few heterotypical cortices (areas of the cortex in which the basic six laminae cannot be recognized) than in homotypical cortex (areas that possess all six laminae)[17, 19].

The combination of histological studies and electro-physiological recordings made with micro-electrodes suggests that the neocortex is organized into vertical units of functional activity (known as cortical columns or modules) traversing the 6 laminae, each unit possessing afferent fibers, internuncial neurons and efferent fibers[18, 19, 20]. With different inputs to the neocortex being processed differently and outputs arising from different neuronal populations, the layering of neurons and fibers within cortical columns provides an efficient means of organizing the input-output relationships of neocortical neurons[18, 16]. A cortical column would fit within a cylinder a fraction of a millimeter in diameter, and its neurons will tend to have very similar electro-physiological response properties, suggesting they form a local processing network[17].

The neocortex contains a large number of functional parts or cortical fields that are specifically interconnected to produce various types of motor, perceptual and cognitive behaviors[21]. Further, most data from animal research indicate that mammals that have neocortices with many functionally heterogeneous parts that are specifically interconnected generally have more complex behaviors[21].

This complexity of the neocortex can partly be attributed to the complex pattern of gyrification that leads to a dramatic increase in the surface area of the cortex, to sulcal folding that allows burying of cortex below the surface, as well as regional cytoarchitectonic variation. As both laminar variability and the number of cortical columns per region are directly related to functional organization, it becomes clear that studies of both are essential to the under-

standing of the function of the cerebral cortex. The number of cortical columns determines the surface area of the cerebral cortex, and is thought to be the major determinants of inter-species differences in neocortical evolution[16].

Total cortical thickness represents the sum of the thickness of the 6 laminae. The thickness of a cortical lamina is a composite measure of neuronal, axonal, dendritic, synaptic, and glial numbers and sizes that may relate to the function of a cortical area. Theoretically, if a change in one lamina was offset by an opposite change in another, total cortical thickness of that particular cortical column may not change. Similarly, if a column increases in total thickness, the change may be due to different changes in different laminae but with a positive sum. The ability to determine the relative contributions of laminar changes to total cortical thickness changes has thus far remained the province of histological research. It is expected that advances in magnetic resonance imaging (MRI) may allow such determination within the next decade or so.

1.2 The Development of The Cerebral Cortex

The fields of developmental neurobiology and psychology are faced with understanding the relation between normal alterations in structure with complex functional changes that occur in infancy, childhood, and through puberty. Whereas different domains of human behavioral development have been described in remarkable detail, we lack a detailed understanding of the essential features of postnatal brain maturation at the structural and molecular level in human beings[24].

The present understanding of the development of the human brain has partially emerged from, and continues to largely rely on incorporating the histogenic constructs that have been identified in experimental animals, primarily rodents[22, 23, 24], and placing that information in the context of the timing of human and other primate ontogeny[24, 25, 26, 27]. This is primarily due to the paucity of descriptive studies in both human beings and other primates, particularly during the postnatal period when substantial brain growth, circuit organization, and myelin formation occur. In addition to this gap in information, the specific molecular and cellular bases for adaptive functional changes that occur in infants and children with typical and atypical developmental trajectories are not fully defined[24].

The following is an attempt to summarize the current state of knowledge:

1.2.1 Prenatal Development

The available evidence shows that the organization of the prenatal cerebral cortex differs substantially from that in the postnatal period with respect to both its cellular constituents and their areal, laminar, and modular arrangement, and their role in changing patterns of neuronal circuits[28, 29, 30, 31]. This dynamically changing state during development produces vulnerable periods that are sensitive to environmental insults because they are dependent on the temporal and regional emergence of critical developmental processes (i.e., proliferation, migration, differentiation, synaptogenesis, myelination, and apoptosis)[32]. It also becomes understandable that developmental disorders of the brain that begin during these vulnerable periods may have wide spread effects on the structural development of the cerebral cortex.

The expansion of the cortex begins at about 56 days of gestation through the first year of life, with the formation of neural connections, the development of unique cytoarchitecture, the growth of dendritic arbors, and the peak formation of synapses extending beyond 350 to 400 postnatal days[24, 34].

The generation of neurons destined for specific layers in the human cortex occurs by cell division in the designated proliferative zones surrounding the lateral ventricles and the achievement of final position by extensive cell migration

in an inside-out fashion (deep-first, superficial-last), all of which begins by the 8th week of gestation[24, 35]. There are exceptions to this limited period of neuron production in the forebrain, such as the rostral subventricular zone, which supplies olfactory structures with neurons through the rostral migratory stream[36] and the dentate gyrus granule cell zone of the hippocampus[37]. Both regions continue to produce neurons in the adult primate[24]. The adult production of neurons destined for the neocortex proper is controversial, however, with the most recent data suggesting little if any intrinsic neuron production[33].

Projections from the brainstem enter the cerebral cortex of the human being between 8 and 15 weeks of gestation and thalamic projections at approximately mid-gestation, overlapping with the time that neurons are generated for the cortex proper[39, 40, 41]. A refinement of connections takes place later in gestation, from about 24 to 28 weeks, and that continues into perinatal periods[39, 40, 41]. This period of time marks the onset of the formation of topographic connections that provide information for functionally coordinated output, which can be measured at approximately 28 weeks of gestation[42]. After the restructuring period in the primate cortex, there is an epoch of remarkable growth, from about 34 weeks of gestation through 24 months after birth. During this time, temporary cellular structures (such as the subplate zone of the cortex) begin to die and productive processes (proliferation and migration) decrease in intensity, while processes of neuronal differentiation, axonal growth and synaptogenesis increase in intensity[42]. An example is synapse formation, which begins to peak in this period[34, 42], with neural connections forming at a rate of almost 40,000 synapses per second[42, 43, 44].

1.2.2 Infancy and Early Childhood

Contrary to the relative maturity of the external configuration of the cortex at birth, some histogenic processes are not yet finished. There is hardly any production of cortical neurons at birth and almost all neurons of the newborn cortex have attained their final positions[42]. Remnants of temporary cellular structures continue to disappear. Cytoarchitectonically, at birth all primary (motor, somatosensory, visual and auditory) cortical areas can be delineated on the basis of characteristic lamination pattern or the presence of characteristic cells (e.g., Betz pyramids in the primary motor cortex). The delineation of secondary and tertiary (association) cortical areas is rather uncertain. One of the reasons is that in the newborn the granular layer (prospective lamina IV) is present in all neocortical areas regardless of their future differentiation into heterotypical or homotypical cortex[42]. Furthermore, the elaboration of dendritic trees of the pyramidal cells is ongoing. In addition, a major event is dendritic differentiation of stellate (Golgi II type) local circuitry inhibitory neurons[41]. Synaptogenesis involving axons that have grown into the cortex prenatally continues, with resulting changes in the distribution and chemical properties of the subcortico-cortical pathways. These changes are thought to play a significant role in the perinatal reorganization of the prefrontal cortex[42]. Cortico-cortical connections continue to form postnatally, and a significant redistribution of cortico-cortical axons during subsequent development can be expected[45].

Since the newborn cortex sends and receives some super-numerous axons and contains the vestige of fetal elements, considerable rearrangements in the organization during the early postnatal cortical development takes place[42]. The phenomenon of overproduction of cortico-cortical axons is closely associated with the excessive synaptogenesis during the early postnatal period[43].

The peak of synaptogenesis in the frontal cortex begins around the 8th postnatal month and reaches a maximum at 2 years of age. This corresponds *temporally* to emergence of skilled actions and cognitive functions[42]. After the elimination of some circuitry elements after the 2nd year of life, the prolonged maturation of goal-directed behavior and the protracted emergence of different cognitive functions *correlates temporally* with the developmental plateau of synapse production which can be seen up to 16 years of age[42].

Myelination increases rapidly after birth and continues in most subcortical tracts through the third decade of life[24]. Based on structural imaging studies, myelination of the cerebral hemispheres begins with the optic radiation and occipital white matter at 1 to 2 months before birth and extends to the frontal lobe by 9 months[47]. The molecular signals that are responsible for the initiation of the myelination process remain unclear. However, it is plausible that perinatal insults such as hypoxia or ischemia, which would affect premyelinating cells more than the more mature, myelinating oligodendrocytes, could preferentially disrupt frontal and temporal lobe tracts, with important functional implications in disorders such as cerebral palsy or mental retardation[24].

The overall impact of this developmental pattern on gross brain anatomy is enormous. From birth through to the fourth year of life, brain volume quadruples, cortical synapse counts double, dendritic arbors of many neurons quadruple in extent, volume of cortical pyramidal cells may double or quadruple depending on region and layer, and the corpus callosum nearly triples in size[48]. The growth of the whole brain in general, and cerebral gray matter in particular, continues at a much slower pace in middle childhood. For example, between 2-4 years of age and 6-8 years, frontal lobe and temporal lobe gray matter volume increase by about 20% and 17%, respectively[49]. Between 6-8 years of age and 11-12 years, frontal lobe and temporal lobe gray matter volume increase by only 5% and 10%, respectively[49].

How do these developmental patterns reflect on total cortical and laminar thickness? As far as the available data can demonstrate, a definite answer is difficult, or at least quite complex. From birth to 72 months, each cortical layer of each of the 41 cytoarchitectonic areas studied in one report repeatedly thins and thickens in a wave-like fashion[50]. On average, each layer changes its direction of growth 3.5 times over six age periods from birth to 72 months[50].

1.2.3 Adolescence and Early Adulthood

Synapse elimination occurs late in childhood and in adolescence in humans[44]. It is followed by a much slower decline in synaptic density during the adult years, which in the human data occurs primarily in old age[51, 44]. The synapse elimination that occurs in late childhood and early adolescence is clearly distinct from the much later and smaller magnitude aging changes. The adult value for synaptic density is about 60% of the maximum[51], the timing of which varies depending on the cortical region between 500 to 1600 post-conception days of age[44]. Dendritic development follows a similar growth trajectory (See figure 1). This process of elimination of circuitry elements, often referred to as "pruning", is necessarily associated with reductions in total cortical gray matter, and reflected in both laminar and total cortical thickness.

As for myelination, a curvilinear increase in its extent between the first and sixth decades of life was shown to be present, with a twofold increase between the first and second decades of life and an additional increase of 60% between the fourth and sixth decades[52]. This continuing development of myelination results in an overall positive direction of growth of the whole brain volume, opposing the expected impact of the pruning process. However, with the possible exception of the dorsolateral frontal cortex and the posterior temporal cortex[53], overall brain volume declines from adolescence onward.

1.2.4 Developmental Correlations of Structure and Function

The epigenetic nature of development combines intrinsic forces that drive neuronal growth and elaboration with extrinsic forces that adaptively modify structure and function according to experience. These two complementary forces underlie the remarkable changes in multiple domains of neuro-behavioral capacity from birth through early childhood[24, 48].

Figure 1: **Postnatal changes in number of dendritic spines of large pyramidal neurons of the layer IIIc of the human prefrontal cortex. Solid line shows the number of spines within the initial 200 pm segment of the apical dendrite, while the dashed line shows the number of spines within the initial 50 pm segment of the basal dendrite. N = newborn; M = months; Y = years. [Adapted from [42]]**

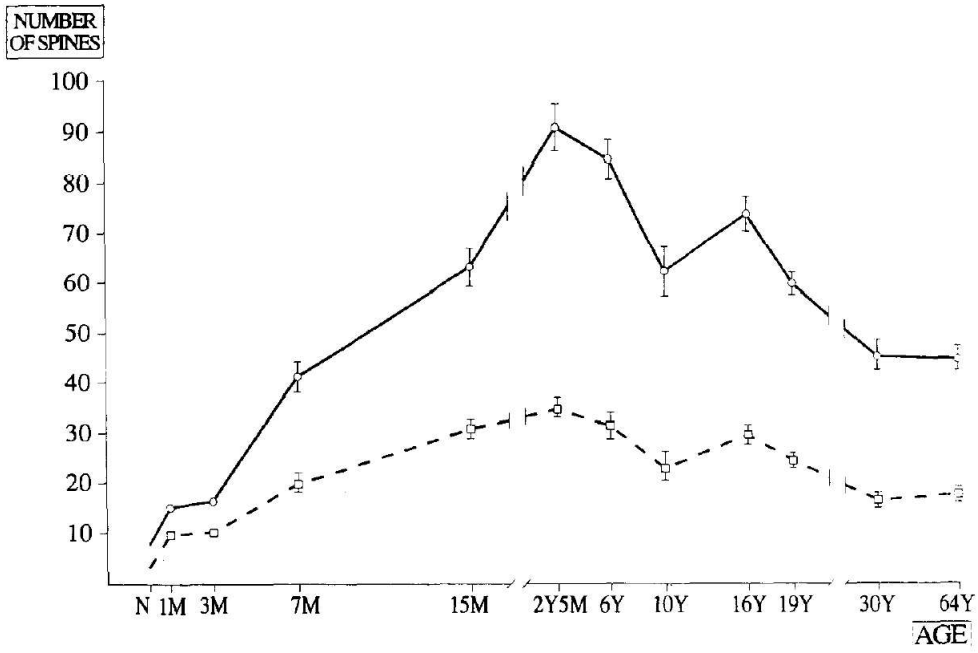

The available descriptive data do not indicate *how* changes in the number of specific cell types or synapses or changes in connectivity are achieved. Changes in connectivity are probably driven by genetic, environmental, and/or a combination of genetic-epigenetic influences. Would early abuse or cognitive deprivation in infancy disrupt the kinetics and the types of synapses that form in the frontal cortex? Although complex functions, such as emotional recognition, can be greatly affected by early experience[46], the relation between experience, synapse type, number, and cognitive capacity in the infant and child remains a field of investigation. Although the peak period of synapse formation does correlate temporally with cognitive and emotional systems developing during the first 2 years of life[24], synaptogenesis does not necessarily correlate with the behavioral and cognitive maturation processes that occur well into childhood. For example, children are unable to perform a simple delayed non-matched to sample task at age 5 but improve dramatically thereafter. In fact, the peak at which children reach their point of best performance corresponds with the period of cortical synaptic pruning[24]. Perhaps this seems counterintuitive, but synaptic pruning during these developmental periods is likely to be essential in the reorganization of local and association circuitry that facilitates integration of information across cortical domains[24]. A summary of some temporal correlations of anatomical and functional developments is presented in table 1.

Correlating cortical thickness changes with functional developmental milestones remains to be done. The reasons for this are likely to be related in part to the disadvantages of post-mortum histological studies of cortical thickness (see a discussion of this in section 3.1 below), to the complexity of cortical development (see figure 2), and the difficulty in establishing accurate temporal correlations in behavior in post-mortum studies. However, some attempts at linking changes in laminar thickness with developments in behavior have been made[50]. Figure 2 is an example of such attempts.

Table 1: **Timing of histogenic brain events and functional milestones. [Adapted from [24, 42]]**

Developmental period	Histogenic milestones	Functional milestones
Early fetal	Progressive differentiation	
Late fetal	Transient organization of connections, Assembly of brain nuclei, cortical structures, major connections;	Fetal movements; fragments resembling goal-directed movements
Birth to 3 months	Transient fine organization of connections; rapid overproduction of synapses; neuropeptide maturation	Transient behavioral patterns; Social orientation (non-discriminating); obligatory looking; voice response
3-6 months	Disappearance of transient patterns; Fragments of skilled movements	Disappearance of transient patterns; Fragments of skilled movements; Face-to-face play; early recognition memory; disengage gaze; modulation of arousal, attention, affect; positive and negative expressions,
8-12 months	Transient fine organization of connections; rapid overproduction of synapses; continued maturation of neurochemical systems	Separation distress, proximity seeking, discriminative preferences for caregiver; early joint attention; working memory and means-end; communication of emotion, acoustic highlighting of words
l-2 years	Peak of associative circuitry production (cortico-cortical)	Maturation of motor and sensory functions, early speech, joint attention
3-16 years	Plateau of synapse production	Protracted development of different cognitive functions

Figure 2: **Development of cortical laminar thickness for the homuncular subdivision of the hand in the primary motor cortex (Brodmann area 4) subserving hand coordination overlapped with the age at which its age-specific behaviors begin. [From [50]] .**

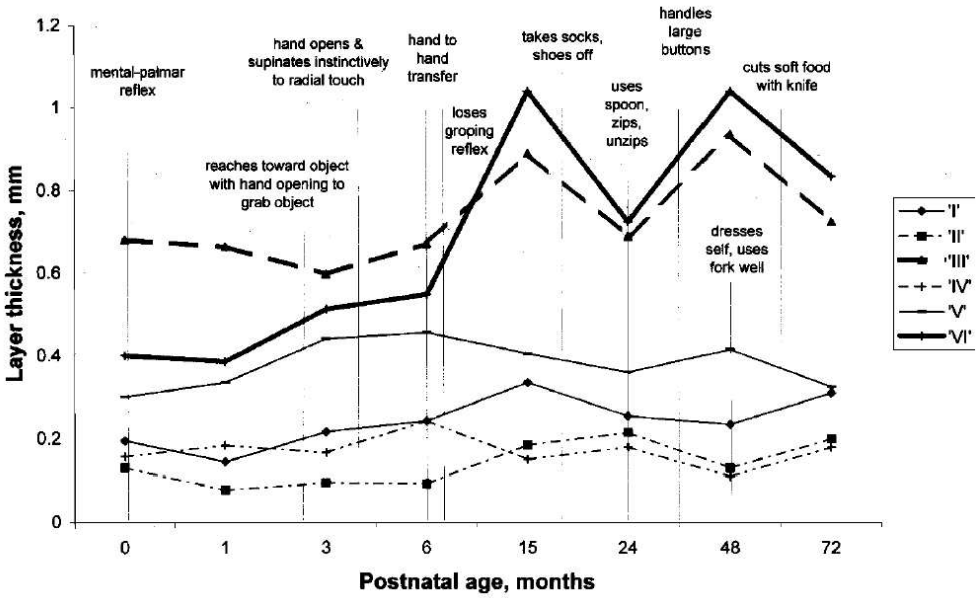

1.3 Cortical Thickness and Pathological Development

1.3.1 General Background

In addition to normal development, cortical changes have been studied in many pathological conditions. There are numerous studies that examined the cerebral cortex in aging and degenerative processes of late-onset[54, 55, 56, 57]. Less is known about developmental histopathological changes in the cortex associated with neuropsychiatric disease, and even less is known about the environmental impact on cortical development. Some examples of the existing data can be found in the study of autism, a neurodevelopmental disorder, and intra-uterine exposure to alcohol, an environmental toxin.

In autism, many components of the limbic system show unusually small neurons that are more closely packed together than those of the age- and sex matched controls[58]. The most consistently involved areas were the amygdala, the hippocampal formation and its closely related entorhinal cortex and the mammillary body. The only exception to this pattern of pathological change was found in the septum, in a part of this area that projects to the limbic forebrain, the nucleus of the diagonal band of Broca. In the younger autistic individuals (less than 12 years of age), the neurons in this part of the septum were unusually large but adequate in number and in the older individuals (more than 21 years of age), they were unusually small and decreased in number[58]. In addition, slightly irregular laminar pattern in the superior frontal gyrus was reported, with clusters of abnormally orientated pyramidal cells[59]. The frontal cortices have been reported to be thickened with increased neuronal density, and the laminar pattern of superior temporal gyrus disorganized[59]. Another change noted in the autistic brain is an unusual pattern of age-related alteration in brain weight (size). The brain weight of young autistic individuals was significantly greater than comparable controls, a finding that is in line with the observed increased head circumference in this population[60].

Fetal exposure to alcohol is neurotoxic. In animal experiments, during the period of synaptogenesis, a single episode of ethanol intoxication lasting for several hours triggers a massive wave of apoptotic neurodegeneration in several regions of the developing rat or mouse forebrain and visual cortex[61]. Ethanol exposure during early postnatal life of rats affected the branching of dendrites in lamina 2/3[62]. In an *in vivo* ultrasonographic study of alcohol exposure during pregnancy, the percent of fetuses with a frontal cortex below the 10th percentile increased from 4% for non-exposed fetuses to 23% for heavily exposed fetuses[63]. And in a study of miscarried human embryos and fetuses of mothers who used alcohol during pregnancy, abnormal development of the cortical laminae occurred in 57.9% of subjects, and the severity was related to the extent of alcohol exposure[64].

1.3.2 Schizophrenia: An Example of Pathologic Cortical Development

Schizophrenia, a severe mental illness that affects almost 1% of the population world wide, is characterized by disorganized thought processes, hallucinations, delusions, cognitive deficits and impaired functioning. Histo-pathological studies of schizophrenia show changes in the cytoarchitectonic organization, cellular concentration and counts, and reductions in laminar thickness and total cortical thickness in a number of brain areas, including Brodmann areas 9 (dorsolateral prefrontal cortex or DPFC), 10, 17, 32 and 46, and in regions such as the anterior cingulate cortex (ACC), the superior temporal gyrus, the Heschl's gyrus, and the entorhinal cortex[65, 66, 67, 68, 69, 70] (see figure 3).

The lack of significant gliosis in the neocortex signifies that degeneration is not an etiological factor[71]. Abnormalities have been reported in pyramidal neurons located in deep lamina 3 of the DPFC. Specifically, DPFC deep lamina 3 pyramidal neurons have been reported to have smaller cell bodies[72, 73], shorter dendrites[74, 75], and fewer dendritic spines in subjects with schizophrenia[74, 75]. Evidence for reductions in neuronal somal size in

Figure 3: **These curves demonstrate the average cytoarchitectonic profile covering the whole cortical depth. The profiles of normals (closed line) and schizophrenics (dotted line) do not differ in shape, however, the gray level index (GLI) values are significantly reduced in laminae III - VI. Different laminae are segmented according to microscopic inspection and local maxima in the first derivative (gray line, bottom). The GLI method is an automated image analysis device, which measures the area percentage of stained perikarya related to the area of the measuring field in histological sections [From [68]]**

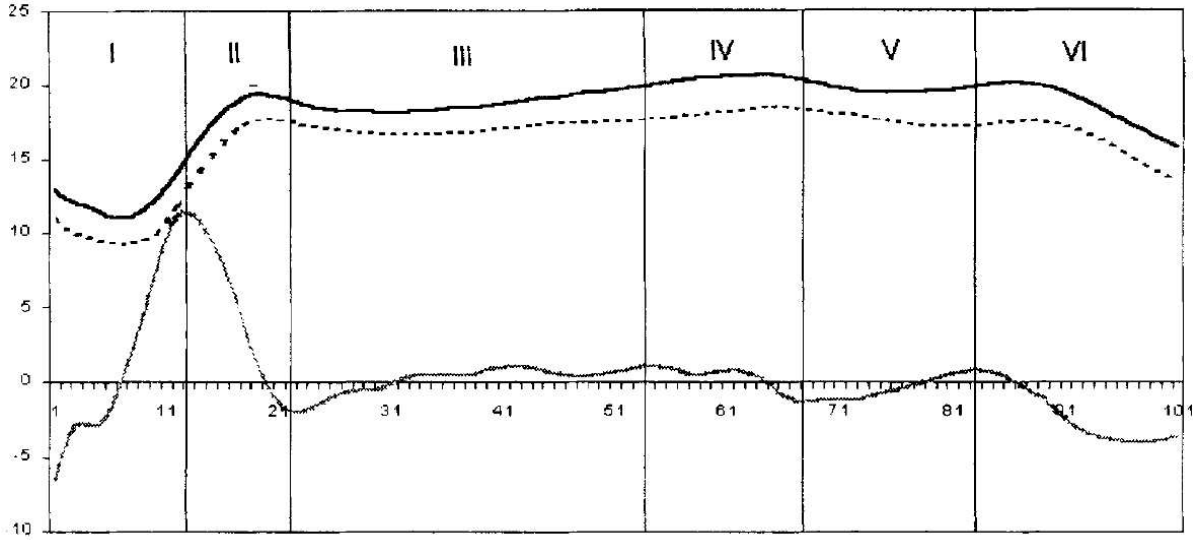

lamina 5 of the ACC, and in right sided neuronal somal size in lamina 3 were also observed in schizophrenia[76]. Temporal lobe abnormalities ranges from a decrease in neuron size in the cornu ammonis (CA) subfields of the hippocampus (CA1-4) [77] to reduced synaptic density in the hippocampus[78] and reduced dendritic spines of pyramidal cells[74]. Investigations of cytoarchitecture have reported an abnormal arrangement and laminar distribution of neurons within the ventromedial temporal lobe which have been interpreted as reflecting unsuccessful migration of neurons during development[69]. Pyramidal neurons within the CA subfields of the hippocampus showed significant variability in their axes of orientation, which was most severe at the interfaces between subfields[79, 80]. This disorganization in the normally uniform alignment of neurons, thought to be a developmentally based migration disturbance, was also found in some qualitative cytoarchitectural studies of the entorhinal cortex[69].

In addition to cytoarchitectural investigations, other research modalities have supported a theory of developmental origin of schizophrenia. Non-specific factors associated with fetal environmental exposures such as prenatal maternal nutritional deficiency, winter birth, birth in an urban environment, and birth and pregnancy complications have been associated with schizophrenia[81]. In fact, the number of pre- and perinatal risk factors is negatively correlated with age of onset until 25 years[82]. Three prospective birth-cohort studies of populations until the ages of 28 and 43 years have differentiated and rendered generally valid the results of earlier retrospective studies into the antecedents of schizophrenia: delayed neuromotor and language development, emotional, behavioral and cognitive abnormalities in childhood and adolescence[83, 84, 85]. Like the sum of pre- and perinatal risk factors, age at walking is negatively correlated with age of onset of schizophrenia[85]. In studies of monozygotic twins discordant for schizophrenia, changes in dermatoglyphic counts that had previously been described in schizophrenic patients were confirmed, providing further evidence of some intra-uterine environmental insults between the fourth and sixth months of pregnancy leading to simultaneous neurologic and dermatologic abnormalities[86, 87, 88].

Presently, many theories explaining the development of schizophrenia exist, but the most popular is the "two-hit"

hypothesis[89]. The first hit or basic requirement is a dysfunctional (mutant) gene, which could have been transmitted via the germ-line or may have been generated by a spontaneous somatic (non-germ-line) mutation early during embryogenesis in the affected individual. Moreover, the genetic contribution may be enforced by the accumulation of an additional mutation in a candidate gene. The second hit(s) comprise multiple environmental factors like viral infection(s), birth complications, and social stressors. The assumption is that (1) the disease-related genes are involved in several key events during neuro-development and/or brain maturation, and (2) that the function of these genes can be modulated by second hit environmental factors[89]. (For an elaboration of this hypothesis and the evidence supporting it, see[90])

2 Cortical Thickness in Brain-Imaging Studies

2.1 Histology vs. Structural Brain-Imaging: A Brief Comparison

Histological measurements of cortical thickness in post-mortum brains suffer from the limitation of cross-sections of the cortical tissue that will align to cortical columns only by chance. Cortical columns are also not always straight or even perpendicular to the pial surface, and may curve along their length. In addition, tissue shape and volume may change drastically from their state in the living organism depending on the methods of preservation and preparation of sections. Therefore, the two-dimensional study of the cortex is hardly accurate in measuring cortical thickness. However, histological analysis allows for breaking down changes in total cortical thickness into its contributing components: such as individual laminar thickness, cellular counts and volumes, and circuitry elements (dendritic arbors and synapses). This advantage enables scientists to test hypotheses that may be at a molecular biological scale. Histological studies of pediatric brains that are informative with respect to CNS development are necessarily scarce, due to low mortality rates across this age range in addition to the rare occurrence of autopsies in this population.

Brain-imaging using currently used MRI technology suffers from the limitation of poor resolution and the difficulties in establishing exact tissue segmentation during periods of dramatic change in tissue water content, such as the first few post-natal months of life. However, these disadvantages were greater in the past than they are presently, and technological advances may ultimately enable image resolution that allows the study of cortical laminar structure to be performed with MRI[91]. On-going research is targeting the difficulties in neonatal tissue segmentation. MR imaging solves the problem of cross-sectioning the cortex with its 3-dimensional protocols, and allows the *in vivo* study of subjects from whom accurate behavioral measurements can be collected. This introduces a vast improvement in temporal resolution over post-mortum histological studies. Therefore, MR corticometry is capable of enriching neuroscience with much insight into the ontogeny of the cerebral cortex. Structural MRI studies are not likely, however, to produce data that can immediately inform us about molecular biological processes. Functional and spectroscopic brain-imaging methods attempt to address that issue, but have their own advantages and disadvantages that will not be discussed in this thesis.

2.2 Developmental Neuroimaging: Current Challenges

Over the past 15 years, innovations in physics and computer science have promoted magnetic resonance imaging (MRI) as an essential tool for investigating the biological substrates of neurological and psychiatric disorders. Requiring no radiation exposure, MRI is now the preferred imaging technique for pediatric populations, but not without ethical caveats[92].

The neurodevelopmental data presented above are all subject of intense neuroimaging investigation. Many psychiatric disorders such as attention-deficit hyperactivity disorder (ADHD, autism, childhood-onset schizophrenia, Tourette syndrome, and early-onset depression have been investigated using neuroimaging techniques (For a review, see[93]). As for normal development, MRI-based anatomical studies have revealed some interesting maturational changes in brain structure. The most consistent findings across these studies include: (1) a lack of any significant change in total cerebral volume after five years of age[94, 95, 96]; (2) a significant decrease in cortical gray matter after 12 years[97]; and (3) an increase in cerebral white matter throughout childhood and young adulthood[98, 99, 96, 100]. Specifically, subcortical gray regions (e.g. basal ganglia) decrease during childhood, particularly in males[94, 96], while cortical gray matter in the frontal and parietal cortices does not appear to significantly decrease until roughly puberty[97]. Total temporal lobe volume appears relatively stable across the age range of 4 to 18 years, while hippocampal formation volume increases with age for females and amygdala volume increases with age for males[95].

2.2.1 MRI challenges in Early Childhood (0-4 years)

Few morphometric imaging studies have included very young children[98, 101]. The main reason for this is the difficulty interpreting MRI data from this population. This is because brain structures rapidly change their biochemical properties and water content during this age period. The most dramatic effects are produced by the progressive myelination of white matter. At birth and for the first 4-6 months of life, signal intensities of gray and white matter are the reverse of those seen in an adult brain, with the signal intensity of white matter being lower than that of gray matter on T1-weighted images and higher than that of gray matter on T2-weighted images[102]. With advancing age, white matter shows a progressive increase in signal intensity on T1-weighted images[102]. On T2-weighted images, high-signal-intensity unmyelinated white matter progressively changes to myelinated white matter of a signal intensity lower than that of gray matter[102]. At birth, the corpus callosum is isointense relative to white matter and progressively increases in signal intensity, so that at age 8 months the corpus callosum has an appearance identical to that of an adult[102].

These progressive changes pose complex challenges for automated MRI processing and analysis tools that depend on the ability to discretely segment brain tissue into gray matter, white matter and CSF based on relatively separable signal intensity ranges for each. For most such segmentation tools, the distinction between white and gray matter will be nearly impossible in the first 3-6 months of life, and begins to function much more accurately by 18 months, when the white/gray distinction approaches that of adult brains. For similar reasons, registering infant MRI data to the standardized Talairach space[103, 104] faces difficulties correctly identifying the brain structures that the registration algorithm bases its spatial orientation on.

Another important difficulty that impacts on corticometric studies in particular, is the fact that sulcal CSF is far less in amount than in the adult brain, leading to a degree of "packing" of cortical gyri. This is problematic given present-day MR technology. When opposing banks of a sulcus are closer to each other than the MR image resolution (most commonly $1mm^3$), segmentation algorithms fail to detect the sulcal boundaries and may fuse adjacent gyri together (what is known as the partial-volume effect[105]). The impact of this effect is of great import if one of the goals of analysis is to generate inner and outer cortical surfaces in order to enable thickness measurements. In addition, toward the end of this age period, gray matter volume is reaching a peak before plateauing and pruning starts. This is reflected in a thicker cortex, which is more difficult to capture by some corticometric algorithms than the normally thinner adult cortex.

The rate of structural change is so rapid, that for a longitudinal imaging study to do justice to brain development

a child would have to undergo frequent serial MRI acquisitions. This poses a logistical and financial difficulty to this form of research.

2.2.2 MRI challenges in Middle Childhood and Adolescence (5-18 years)

Many of the above mentioned difficulties greatly subside during this age period. Signal intensities continue to change. For example, in T2 weighted scans, the signal intensities in the white and deep gray matter decrease rapidly in the first decade of life and then gradually reach a plateau after the age of 18 years[106]. Most available segmentation algorithms would be able to correctly identify gray and white matter and CSF with little difficulty. However, the problem of the partial-volume effect stubbornly persists as the amount of CSF in sulcal spaces increases very slowly throughout the life span. The rate of structural change is decidedly slower in this period. Therefore, fewer MRI acquisitions with longer intervals would suffice in a longitudinal study of brain development.

2.3 Possible Approaches to MR Corticometry

We are introducing the term "corticometry" in order to refer to all morphometric studies of the cerebral cortex. These may include studies of surface area, folding, gyrification and sulcal patterns, cortical volume, cortical thickness and surface reconstruction, lamination, and modulation (cortical column formation), among others. Anatomical MR corticometry is the method addressed in this thesis, but functional MR and histological approaches can be subsumed under the global term "corticometry". Cortical thickness will be the research area this thesis will focus on. In order to be able to measure cortical thickness, accurate reconstruction of cerebral cortical surfaces from MR images is essential. This is dependent on many algorithms involved in post-acquisition processing of MR images. The outcome is a computed hollow 3-dimensional object that represents the folded 2-dimensional white matter surface (WMS) of the cortex, which lies within another hollow 3-dimensional object representing the folded 2-dimensional pial surface (PS) of the cortex. Each surface represents only the boundary between two tissue classes, and is therefore without thickness. Each of these surface sheets may be triangulated to become a polygon mesh of thousands of small triangles, and each node in the mesh is referred to as a "vertex". When the corticometric study in question is utilizing properties of these vertices for purposes of inter-subject comparison, we will refer to the method as "vertex-based". This is in counter-distinction from voxel-based MR-image analytic methods, the unit of which is the 3-dimensional "volume elements" generated from the image.

2.3.1 Manual Segmentation

The delineation of cortical surfaces manually, although not impossible, is prohibitively time-consuming. This is especially true when populations need to be compared, given that the surface area of the PS of a single brain was estimated (manually) to be between 200,000 and 248,000mm^2[107]. However, the problem becomes more manageable if only a well defined area of the cortex is to be segmented. This region-of-interest (ROI) approach can only be implemented in spatially localized cases in which the image plane is orthogonal to the cortical surface throughout a region of interest, allowing the measurement of thickness to be accomplished from slice data (For an example of cortical thickness measured manually in an MR study, see[108]).

Apart from the extraction of cortical surfaces, partial or complete manual segmentation may be necessary in handling problems for which computational methods don't exist or are inadequate. One example is the problem of choosing anatomical landmarks in infant brains to be the base for the algorithm that registers the volume to

standardized stereotaxic space. The lack of clear signal-based tissue-class distinction in this age group was discussed above, and necessitates the use of *a priori* knowledge by human raters.

Manual segmentation may serve as a tool for validating automated methods. Since automated methods can only approximate the performance of an expert in neuroanatomy, some manual segmentation is required to detect some errors in these automated algorithms and be able to modify them. The problem is that manual segmentation introduces human error. Human error can be unique to the person performing the task and to the time the task was performed. These factors require additional validation steps such as intra- and inter-rater reliability measurements.

2.3.2 Computational Methods

As opposed to manual segmentation, automated and semi-automated computational methods allow for the study of large datasets and are more time-efficient. They also limit the issue of human error, and replace it with computational errors. The main advantage of this is that computational errors are much more likely to be uniform or systematic in degree and frequency. Since the main disadvantage is usually related to accuracy of the computational method in contrast to manual segmentation, and since inaccuracies are likely to be systematic and/or randomly distributed on larger datasets, the overall negative impact is likely to be small. How well an algorithm performs depends to a great deal on data quality, and on robustness and stability of its programing code in dealing with the vast biological variations it is likely to encounter in the data.

2.4 The Methodological Challenges of Automated Cortical Thickness Estimations

2.4.1 Extraction of The Surfaces

The inherent limitations of MR image under-sampling, lack of contrast, intensity bias, and noise have made the segmentation of fine anatomic details a difficult task. This problem is nowhere more evident than in the highly convoluted human neocortex. Until recently, the accurate extraction of the cortical surface has been an exceedingly difficult task[109]. This is primarily due to the partial volume effects encountered in folded gyri and deep sulci[109, 1]. The methods that currently exist for identifying the cortical surfaces attempt, with varying degrees of success, to overcome this difficulty. They are classified into bottom-up approaches using edge detection and top-down approaches using deformable models.

2.4.1.1 Edge Detection: The "Bottom-Up" Approach It is possible to segment, match and track images of anatomic structures by exploiting constraints derived from the image data. This purely bottom-up approach, exemplified by the "Marching Cubes" algorithm[110], although has high resolution, is unable to cope with noise in the data and has no means of limiting surfaces to accurate topology[109, 1]. These factors limit its utility in corticometric studies.

2.4.1.2 Model-Based Deformable Surfaces Techniques Top-down approaches are methods that depend on the use of *a priori* knowledge about the location, size and shape of anatomic structures in the image. Deformable models, a vigorously researched model-based approach to computer assisted medical image analysis, have the added potency that stems from their inclusion of aspects of both the bottom-up and the top-down approaches[111]. Deformable models are capable of accommodating the often significant variability of biological structures over time and across different individuals[111]. Furthermore, deformable models support highly intuitive interaction mechanisms that allow anatomists to bring their expertise to bear on the model-based image interpretation task when necessary[111].

Many algorithms based on the deformable models concept are presently in use to extract cortical surfaces and calculate cortical thickness. A well known example is the FreeSurfer program[112, 113, 114], which initially finds the WMS by classifying brain tissue into its components in voxel-space then locating the white/gray matter boundary, and then fits a smooth WMS deformable model. Once the WMS is produced, the program then expands a deformable surface toward the PS. This method has already been used with success to measure cortical thickness maps in Huntington's disease[115], schizophrenia[116] and multiple sclerosis[117]. At least three other variations on this theme have also been in use[118, 119, 120]. These methods vary in their topological correctness, ability to cope with partial volume effects, and capacity to limit self-intersection of produced surfaces[1, 109].

A method introduced at the MNI, known as Anatomic Segmentation using Proximities (or ASP)[109], uses a topology-preserving deformation model, and automatically identifies the WMS from previously segmented (tissue-classified) volumes. It then generates the PS of the cerebral cortex by expanding a deformable surface while forcing the cortical thickness to lie within an *a priori* defined anatomically-plausible range of values and explicitly preventing self-intersection of the generated PS. These and other added constraints were designed to reduce the impact of partial volume effects. ASP has been successfully used in our lab as part of an early version of a corticometry pipeline[121], and has resulted in studies of cortical thickness in normal aging[122], Alzheimer's Disease[123], and epilepsy[124].

Although ASP is either more robust or at least equally robust when compared to the above mentioned methods, its dependency on thickness constraints to manage the partial volume effect leads to failures in capturing the full thickness of the cortex in pediatric populations and in conditions leading to increased thickness (such as cortical dysgenesis) or much thinner cortices than the algorithm allows[1]. In fact, in earlier experiments with pediatric populations (see section 1.3), cortical thickness extraction was more accurate in the childhood-onset schizophrenia (COS) group than in the normal controls. This was due to thicker cortices on visual inspection in the normal controls, and has resulted in a loss of power to detect differences between the two groups. A modification of ASP has recently been introduced: Constrained Laplacian-based ASP (CLASP)[1]. The improvement introduced by CLASP is a result of (a) abandoning the thickness restraint, (b) utilizing information produced by a partial volume classification algorithm already in use in our lab[125] to inform the algorithm about the location of PS, partly by producing a skeleton of extra-pial CSF[126] that becomes a rigid boundary beyond which no pial surface exists, and (c) by modifying the method of expansion of the deformable surface that eventually generates the PS. This latter component is a major advance from the usual approach of finding the nearest boundary. Instead, the PS-generating geometric deformable surface expands from the WMS toward the skeletonized CSF along tracks defined by gradients produced by a Laplacian map. This Laplacian map provides smoothly increasing potential surfaces between WMS and skeletonized CSF. Its gradient produces an expanding route for the PS, and guarantees topological preservation (see figure 4)[1]. The improved accuracy in capturing healthier and thicker cortices resulting from the introduction of CLASP should increase the likelihood of detecting group differences. This will enable the application of vertex-based corticometric studies of psychiatric populations in general and pediatric populations in particular. Note that in ASP and CLASP, the WMS is a polygonal mesh. When the deformable surface expands outward toward the PS, it starts with an identical polygonal mesh. This leads to a situation were each vertex on the WMS has one corresponding vertex on the PS. The total number of vertices on each surface is identical to that of the other. The importance of this fact will become clear in the following section.

2.4.2 Definition of The Thickness Metric

Studies in our lab were performed to define the most appropriate measurement of thickness in corticometric studies[121]. This was necessary, as there was no widely accepted definition of thickness, and different groups used different met-

Figure 4: **Deformation model using (a) the distance map and (b) the Laplacian map.[From[1]]**

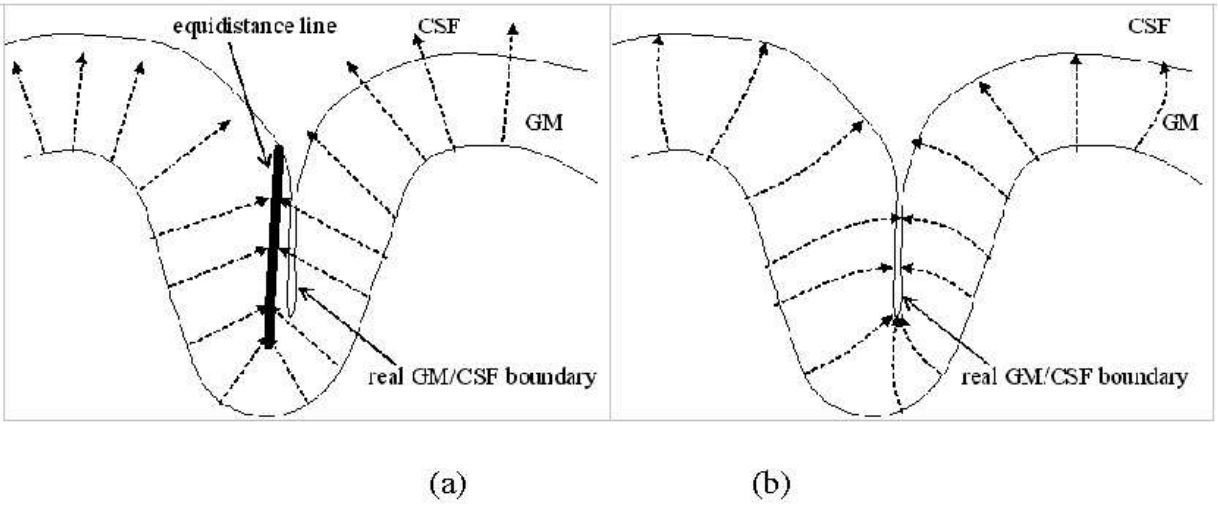

rics. Six possible metrics were compared: (1) distance along the surface normal (t_{normal}), (see [109] for an example); (2) distance along an iteratively computed surface normal ($t_{layered\text{-}normal}$); (3) distance toward the nearest point in the opposite surface (t_{near}), (see [109] for an example); (4) distance along a line that is the average of the nearest point measured from each side ($t_{average\text{-}near}$), (see [17, 114] for examples); (5) distance between the corresponding, or linked, nodes on each surface (t_{link}), (see [109] for an example); the correspondence being a product of the mechanism producing both surfaces; and (6) the distance dictated by the Laplacian equation ($t_{laplace}$), (see [127] for an example). Although both the t_{link} and the $t_{laplace}$ methods were superior to the other 4 metrics in their specificity and sensitivity, the t_{link} metric had greater robustness than the $t_{laplace}$ metric[121]. As a result of these experiments, the t_{link} metric was chosen to be the default metric for measuring cortical thickness in our lab's corticometry pipelines.

2.4.3 The Statistical Challenges

2.4.3.1 Typical vs. Average effects A major impediment in neuroimaging research is cost. Additionally, longitudinal research for anatomical studies often requires intervals of months or years between measurements. Compounding these factors in pediatric studies is the practical difficulty inherent in scanning young children, especially when mental pathology is involved. These caveats result in the small sample sizes observed in most neuroimaging studies. The problem of deciding on appropriate sample sizes is also complicated by the inherent properties of the data and the kind of statistical inferences resulting from them.

When the research aim in a longitudinal design is to detect effects that reflect *qualitative* aspects of normal anatomy in a sample of healthy individuals, i.e. "typical effects" that are likely to be present, fixed-effect statistical models can be used to address the hypothesis[128]. However, when the aim is to measure *quantitative* metrics that may be different in some populations than others, i.e. effects that "on average" are of different quantities in the studied groups, random-effect statistical analysis is more appropriate[128]. In corticometric studies, the presence or absence of temporal lobe cortical thinning over time is a qualitative question. If one would like to know if it was typical of normal individuals for whom a number of measurements exist per subject, the inference made would still be valid if the occasional subject did not have cortical thinning but most subjects do. In such a situation, fixed-effect models applied to relatively small samples may allow correct inferences. However, when the question is whether

the temporal cortex in schizophrenic subjects thins more rapidly than normal subjects, the quantitative nature of the question and the need to infer that the effect will always be true given enough subjects dictates the use of random-effects analyses, which will require much larger samples to reach correct inferences[128].

2.4.3.2 Whole-Brain vs. Region of Interest Analysis In a typical MR volume acquired at the resolution of $1mm^3$ (which is the volume of each voxel), there would be around 1,000,000 voxels in that single volume. Whole-brain voxel-based morphometry will involve that many voxel by voxel comparisons. In our lab, our polygonal meshes, produced by ASP or CLASP, give rise to surfaces with 81,924 polygons each, and thickness is therefor measured at each of 40,962 vertices. Vertex-based comparisons are not as numerous as voxel-based ones, and corticometry concerns itself only with the cortical mantle. These numbers would have been prohibitive had it not been for the presently available computational capabilities in brain-imaging centers. In addition, having reliable automated tools to perform the image analysis on large datasets is only a recent luxury.

Region of interest (ROI) analysis was until recently the logical approach in MR morphometry. These regions are defined based on their cytoarchitectonic classification (Brodmann area) or by major anatomical landmarks. Most processing methods are either entirely manual or semi-automated. Typically, the ROI would be manually segmented by operators that trace the anatomical boundaries of a brain structure. Not only is this subject to human error, but *a priori* definitions of structures cannot completely account for natural anatomic variability and become more complicated when pathology exists. When standard normalization techniques are used, accommodation of inter-subject variability is only partial[129]. When full-brain normalization procedures are used, there remains a considerable degree of residual variability in the shape and location of regions defined based on anatomical markers[129].

The main advantage of ROI designs is that the number of comparison units is small and the power for detecting small effect sizes is high. This has raised the question of whether inferences from comparisons at such small scales are as valid as they seem. It is quite probable that detectable effects in an ROI approach may not be detected in a well-designed whole-brain approach. The reverse is much less probable.

2.4.3.3 The Problem of Multiple Comparisons When a decision is made about the validity of a single comparison, errors can take place: a true null hypothesis may be rejected, or a false null hypothesis may fail to be rejected. In most experiments, the validity of multiple comparisons has to be decided. In such situations, chances are a true null hypothesis will be rejected. The challenge for any multiple comparison procedure is to satisfy two conflicting requirements: reduce the risk of rejecting a true null hypothesis, but maintain the likelihood of confirming the alternate hypothesis by detecting an experimental effect if it exists[130]. A number of methods are currently in use in neuroimaging research that offer varying degrees of correction for multiple comparisons. A very short summary of the main ones is presented below.

Bonferroni Correction This is a commonly used *familywise error* correction method. Familywise error is defined as the probability of falsely rejecting any of a series of null hypotheses applied to the data. The premise of the Bonferroni correction is simple, and all that needs to be done is to replace the threshold for significance (α_1) with the level α_1 divided by the number of tests being performed (k). i.e. α_1 is replaced by $\alpha_2 = \frac{\alpha_1}{k}$.

Although the Bonferroni correction has strong control of Type I errors, it is too conservative in practice with neuroimaging data, particularly with whole-brain approaches. It will likely eliminate both false and true positives, and usually leads to unnecessary loss of statistical power[131].

Random Field Theory The three-dimensional Gaussian random field theory (RFT) method[132, 133, 134, 135, 136] is a familywise error correction method that takes into account the fact that test elements (voxels or vertices) are inherently correlated spatially to adjacent elements for both biological reasons and as a result of the filters imposed on raw intensity data in order to construct images. This spatial coherence is related to the full-width at half-maximum (FWHM) of the reconstruction filter, which is much higher than the scanner resolution. It presupposes that the data is parametric, that they share certain topological characteristics (such as the Euler characteristic), and requires that they are smoothed along a Gaussian kernel. Utilizing these characteristics and the Gaussian smoothing kernel, the method estimates a number of "resolution elements" (*resels*) that are, in simplistic terms, clusters of spatially correlated voxels or vertices. Resels then become the sampling unit of the dataset. These resels or clusters of voxels have dimensions equal to the effective FWHM of the reconstructed image in each dimension.

The effective reduction of the impact of multiple tests is dependent on the the smoothness of the data. The less smooth, the more conservative the threshold becomes. This is because RFT is supposed to be "exact" if the assumptions of the method are all correct within the dataset. Since data only approximate these assumptions usually, the RFT may be more or less conservative accordingly.

A minor variation of this method is now available for use in corticometric studies[135]. Although the original RFT implementation for cortical surfaces used a 3D smoothing kernel which can be problematic, this was later resolved by the introduction of a surface-based smoothing kernel[137]. Another complication is the non-isotropic nature of surface data. To deal with this issue, the effective FWHM (eFWHM) is estimated along the topography of the surface.

Non-parametric Permutation Testing Requiring only minimal assumptions for validity, nonparametric permutation testing[138, 139] provides a flexible and intuitive methodology for the statistical analysis of neuroimaging data. It comes, however, at a significant computational expense, and it is difficult to account for temporal autocorrelation. At present, it appears that this method is seldom used to correct for multiple comparisons in anatomical neuroimaging studies. For this reason it will not be elaborated upon in the present thesis.

False Discovery Rate Procedure In most experiments, the aim is to make a discovery: to reject a null hypothesis. When an experiment involves a family of comparisons, a mistaken discovery is more likely to be made. The false discovery rate (FDR) procedure [140, 141] does not control the familywise error, but the false discovery rate. Essentially, only among the elements (voxels or vertices) that do show an effect, the expected fraction of null hypotheses rejected mistakenly is the FDR. The way this is achieved is by using a thresholding method that adopts to the properties of the given dataset.

The FDR does not take into account the spatial coherence of the data. In fact, at least theoretically, the smoother the data the more conservative FDR becomes[141]. The advantage of the FDR method over the RFT method is that it increases sensitivity to detect effects in the data, at a reasonable and controlled compromise of false positives. Its disadvantage is that detected results will have a definite proportion of false positives.

When the FDR method was studied in our lab for robustness, the gain in true positives detected was much greater than the predicted false positives. Similarly, a large drop in false negatives resulted[121]. Over the past couple of years, experience in the lab with this method has been very encouraging.

2.4.3.4 Statistical Power Most neuroimaging studies are interpreted without accurate estimates of statistical power. Instead, the notion of power is based on what has been detected in previous studies[131]. This lack of a systematic

and widely adopted method for calculating power likely contributes to limited reproducibility of results across similar experimental studies. This is because reported data may be false positive, and undetected findings may be a result of conservative statistical models, when the power of the compared studies cannot be determined[131].

3 Proposed Project

The neurobiology of the cerebral cortex, some of which was summarized above, illustrates the dynamic status of what might well be the part of the brain that makes us human. Not only is the cognitive, psychological and motor development of the individual linked to this dynamically changing structure, but major morbidity to the individual and cost to society can be incurred from disruptions to the neocortical developmental trajectory. The neuroimaging methodologies available presently have great potential to enrich the understanding of the ontogeny and pathology of the neocortex.

3.1 Hypotheses

The core hypothesis is that the neocortex follows predictable trajectories of development that manifest in measurable cortical thickness changes over time in the average normal individual, but is sensitive to both environmental insults and developmental neuropsychiatric disorder.

3.1.1 The Normal Development of The Cerebral Cortex

The neocortex grows progressively thicker on average, but will have regionally specific rates of growth, from birth till an age between 2 and 4 years (target age being regionally specific). Following this peak of cortical thickness gain, a mildly decremental plateau ensues till mid-adolescence (target age being regionally specific) which then gives way to a moderately decremental slope that continues well into adulthood.

3.1.2 The Impact of The Environment on Cortical Development

In comparing two groups of well-matched adolescents in a cross-sectional design, the group exposed to adverse intrauterine environment resulting from maternal cigarette smoking will demonstrate differences in cortical thickness maps that are significant and are correlated to the extent of exposure.

3.1.3 The Impact of A Developmental Disorder on Cortical Development

In three different experiments, schizophrenic subjects of all ages will demonstrate significant differences in cortical thickness maps, and significantly different trajectories of cortical thickness change over time that are correlated to the manifest clinical symptomatology.

3.2 Specific Aims

This project primarily aims to demonstrate in four separate experiments that there are regionally specific developmental trajectories of cortical thickness that can be significantly influenced by exposure to adverse intrauterine

environments resulting from maternal cigarette smoking, and by the insidious development of schizophrenia. A secondary aim that would be achieved by the pursuit of the primary aim, is to illustrate the extensive potential of the *C*orticometric *I*terative *V*ertex-based *E*stimation of *T*hickness (CIVET) pipeline (developed at the MNI) when applied in a whole-brain approach, in the study of the development and pathology of the cerebral cortex.

3.3 Procedures

3.3.1 The Methods: A Description of CIVET

CIVET is a carefully assembled series of inter-dependent algorithms, or pipeline, that is designed to prevent faulty output from going further in the process that eventually enables corticometric analysis of MRI images. The pipeline is also designed to be able to handle large datasets simultaneously. At present, a stable version of CIVET (version F-1-a) is operational and will be the method used for this project. CIVET includes 35 different steps that may need 80 to 160 computation hours per volume to be completed. The major processes performed are as follows:

1. Correction for RF intensity non-uniformity artifacts using the N3 algorithm[143];
2. Linear registration to the ICBM 152 average brain in MNI-Talairach space using the MNI_AutoReg software package[104]. The linear transform uses a 9-parameter affine process (translation, scaling and rotation);
3. Tissue segmentation into three classes: white matter, gray matter and CSF (also referred to as "classification") by discrete classifier that uses advanced neural network methods (the INSECT algorithm)[144];
4. Regional brain segmentation (anatomic labeling of major brain organs) according to a 3-D probabilistic map[145, 146, 147], using the ANIMAL algorithm[104];
5. Partial-volume (fuzzy) tissue classification and generation of a skeleton for the CSF[125, 1];
6. CLASP[1, 109] (see detailed description in 3.4.1.2 above);
7. Inter-subject non-linear surface registration of the WMS[148] – (optional);
8. Reverse transformation of volume (for purposes of thickness measurement in native-space)[149] – (optional);
9. Using the t_{link}metric, thickness at each vertex is calculated (optionally twice, standardized and native thickness)[150, 121];
10. Blurring of cortical thickness maps using a surface-based smoothing kernel[137].

Once CIVET is done processing the data, two additional steps (statistical analysis and visualization) follow. Statistical analysis utilizes a combination of the R statistical package[151] and MATLAB[152] to generate statistical models (frequently multivariate analyses and linear logistic regression models) and significance thresholds (via FDR and/or RFT methods). Visualization of CIVET output files is achieved with MNI-Register and MNI-Display (developed at the MNI in 1993 by David MacDonald[150]). Visualization of cortical thickness maps and statistical analysis output is achieved with Brain-View (developed at the MNI in 2000 by Jason Lerch. See examples of this in [149, 153, 121, 122, 123, 124]).

3.3.2 Methodological Contributions to Corticometric Studies

This thesis will be primarily focused on the developmental and clinical *application* of existing methods. However, the intimate dependency of automated measures on their biological *a priori* assumptions creates situations that can only be resolved by both a working knowledge of methods by biologists, and a degree of involvement in methodological development. The first two contributions below will be shared efforts with Richard Webster, Reza Forghani , and Louis Collins. The third task has largely been completed.

3.3.2.1 Manual Registration of Infant Data Given the difficulties of poor tissue contrast on MR images from very young children, manual interventions must inform and/or precede automated processing of the data. Fifty eight MRI acquisitions from children ranging in age from one month to five years of age (from the NIHPD Project) will be manually aligned by the following steps:

1. Designating a set of tag points that span the brain lobes and central structures and then manually identifying them on each of the volumes.
2. Inter- and intra-rater reliability measurements of the manual tagging procedure will be performed for all three raters.
3. A variant of the existing inter-subject registration algorithms[104] will be trained to use these manual tags to achieve initial registration
4. Automatic registration to Talairach space as a final registration step.

This process will be further examined for the possibility of full automation by Dr. Louis Collins and his students. A detailed report of the method and its outcome will be published.

3.3.2.2 Validation of Classification Algorithms in Pediatric Data Using the same dataset as in 4.3.2.1, manual validation of the classification (tissue segmentation) algorithms that will be in use for this population will be performed. The classification algorithm used will probably need to be modified to include more than the classical 3 discrete tissue classes. In order to improve the performance of automated algorithms on infant MRI volumes that has lower contrast between tissue classes, an attempt to force the recognition of subclasses may be necessary. Gray matter may be sub-classified into cerebral cortical, cerebral deep and cerebellar gray matter if intensity histograms allow such a sub-classification. Similarly, white matter may be sub-classified into cerebral and cerebellar, and each into unmyelinated, varying degrees of myelination and fully myelinated. Classes for vasculature may be of use as well. Adding spatial *a priori* knowledge may be useful. These modifications will be performed by Dr. Louis Collins and his students

Ultimately, the tissue classifier is likely to be quite different from what is presently in use. Validation will proceed as follows:

1. A randomly selected large number of voxels per hemisphere in each volume will be examined manually, contrasting the designated tissue class generated by automated classification with expert opinion.
2. Inter- and intra-rater reliability measurements of the manual classification procedure will be performed for all three raters.

3. The task of computing validity will be broken down to three parts: (a) validity of classification in and around the cerebral cortical mantle, for which I will be the major contributor; (b) validity of classification of deep cerebral and cerebellar gray matter, for which my contribution will be secondary; and (c) validity of classification of white matter, for which my contribution will be secondary.

At least three reports are expected to be published from this work.

3.3.2.3 Measuring Cortical Thickness in Native-Space Automated processing of MR images is heavily reliant on the spatial normalization of the data that allows voxel-based comparisons between subjects. This normalization process enables the production of statistical parametric maps for group comparisons[154]. This is achieved by linearly registering each image with the same template image. The template image is usually aligned to the 3D Talairach stereotaxic coordinate system (commonly referred to as Talairach space). This spatial standardization is supposed to preserve *relative* topology within the brain, and allow for inter-subject differences in topology to be uninfluenced by whole brain volume or spatial orientation artifacts. This method has now become a gold standard in whole-brain approaches to morphometry.

The above described spatial normalization was developed long before cortical thickness analysis became feasible. Given the unique biological properties of the cortex that are the result of its cytoarchitechtonic and modular structure, the 2D metrics of thickness and surface area, as well as its sulcal and gyral patterns, are of much greater importance than the metrics generated by voxel-based methods, such as volumes and gray matter density (an ambiguous metric with unclear biological correlates in the cerebral cortex). In addition, assumptions about standardization that may apply to deep brain structures and to white matter may not necessarily be correct for the neocortex. Essentially, when it comes to cortical thickness, the absolute values are at least as informative as the relative values. In some clinical populations, it can be argued that the absolute values of thickness are the only way to go.

Examples of situations that may challenge the spatial normalization paradigm would be when a group with a mixture of both global cortical thinning and second order thinning in a few isolated cortical regions, is compared with a normal population. A good example for this is schizophrenia. As a result of performing the study detailed in 4.3.5.3 below (see [153]), the opportunity became available to test this question of spacial normalization in cortical thickness studies. This effort has resulted in the inclusion of a reverse registration code in the present version of CIVET.

The technical problem that required a solution was that extraction of surfaces was reliable only when done on volumes classified within standardized space. In addition, intersubject comparison would be impossible without alignment to coordinate system that enables an element by element comparison. The solution to this hurdle was reached by the following compromise: (1) Volumes are all processed normally by CIVET, (2) Once CLASP has generated the cortical surfaces in standardized space, a surface based non-linear inter-subject registration of the surfaces is performed[148]. This results in a one-to-one registration of all vertices across subjects. (3) This registered surface is then allowed to undergo a reversal of the volumetric transform. This transfers the registered surfaces back to native space while retaining the spatial information necessary for inter-subject vertex-based comparisons.

The mean cortical thickness in schizophrenic subjects was shown to be lower than that of normal controls when the comparison is made in native space, and to be no different when the comparison is made in standardized space[149]. Regional differences in statistical thickness maps become attenuated when the comparison is in standardized space, compared to native space. What this means is that spatial normalization, in addition to eliminating the global differences that are developmentally informative, has biased against the detection of real regional differences[149]. (Compare figure 5 with figure 6).

Table 2: **Objective 2 Longitudinal and Cross-Sectional Sampling Strategy [From [156]]**

Age (months):	0	3	6	9	12	18	24	30	36	42	48	60	72	
Sample Size*														Child-scans Subtotal
Cohort 1	24	19	15	12	10									80
Cohort 2			22		18	14	11							65
Cohort 3						20	16	13	10					59
Cohort 4								18	14	12	10			54
Cohort 5											16	13	10	39
Cross-sectional Subtotal:	24	19	37	12	28	34	27	31	24	12	26	13	10	297

* assumes 20% attrition between imaging occasions regardless of their irregular temporal spacings

3.3.3 Normal Growth Trajectories of Cortical Thickness

The NIHPD project is a multi-site study that is collecting a representative sample of normal, healthy children aged 0-18 years in order to provide longitudinal MR and behavioral data that enable the investigation of brain maturation in relation to behavioral and cognitive development[156]. Dr. Evans is the principal investigator of the data coordination center (DCC) at the MNI.

My involvement in the study will be restricted to the statistical analysis of cortical thickness data, and correlations of this aspect of brain anatomy with behavioral maturation. The objective will be to develop:

- A vertex-based normative age-specific atlas of cortical thickness;
- Regional growth-curve analysis, both univariate and multivariate;
- Brain-behavior correlates, through the inclusion of behavioral data as regressors in the growth-curve models.

These goals will be achieved through the use of the CIVET pipeline described above, followed by the necessary statistical analyses.

The following 2 subsections briefly describe the subjects that will undergo the study. For details of the overall project protocol, MR acquisition protocols, and behavioral instruments used, please refer to the project's documentation[156].

3.3.3.1 The NIHPD Project: 0 to 4 1/2 Years This part of the project is referred to as "Objective 2". Approximately 85 children will participate in Objective 2, with equal distribution across age strata and gender. Each recruited subject will undergo a battery of behavioral measurements and an extensive MR imaging protocol at each visit. There will be between 3 to 5 visits per recruited subject over a duration of 12 to 24 months, depending on the age stratum of the subject. See Table 2 for details of the sampling plan. The total number of child-scans for Objective 2 is expected to be a minimum of 277 (based on an assumption of 20% compounded between-visit attrition)[156].

Table 3: **Objective 1 Longitudinal and Cross-Sectional Sampling Strategy. [From [156]]**

Age (years):	5	6	7	8	9	10	11	12	13	14	15	16	17	18	19	20	21	Child-Scans Subtotal
Sample Size*																		
Cohort 1	55		44		35													134
Cohort 2		55		44		35												134
Cohort 3			55		44		35											134
Cohort 4					55		44		35									134
Cohort 5							55		44		35							134
Cohort 6									55		44		35					134
Cohort 7											55		44		35			134
Cohort 8													55		44		35	134
Cross-Sectional Subtotal:	55	55	99	44	134	35	134		134		134		134		79		35	1072

* assumes 20% attrition between imaging occasions

3.3.3.2 The NIHPD Project: 4 1/2 to 18 Years This part of the project is referred to as "Objective 1". Approximately 440 children will participate in Objective 1, with equal distribution across age strata and gender. Each recruited subject will undergo a battery of behavioral measurements and an extensive MR imaging protocol at each visit. There will be 3 visits planned for each subject over a 4-year period. See Table 3 for details of the sampling plan. The total number of child-scans for Objective 1 is expected to be a minimum of 1072 (based on an assumption of 20% compounded between-visit attrition).

Recruitment has been completed, and so has the first visit for all subjects. The second visit stage has begun.

3.3.4 Impact of Prenatal Environmental Toxins on Adolescent Cortical Thickness

Results from the National Longitudinal Study on Children and Youth (NLSCY) indicate that 23.3% of Canadian women smoke during pregnancy[155]. Of these women, 84% smoke throughout pregnancy. Rates of daily tobacco use among pregnant women is distributed in the following manner: 65% smoke between 1 and 10 cigarettes a day; 34% smoke between 11 and 25 cigarettes; 1% smoke more than 25 cigarettes[155].

Dr. Evans is a collaborator in a project (PI: Dr. Tomáš Paus) titled: "Long-term consequences of prenatal exposure to maternal cigarette smoking on brain structure, function and mental health in adolescence: Role of genes and environment in brain development". At present, I'm at the early phases of involvement in this study. The study sample constitutes two groups of adolescents from the geographically isolated population of the Saguenay-Lac-Saint-Jean region of the Provence of Québec. The groups are well matched, but differ in that one group had been born to mothers that smoked during pregnancy.

These adolescents have undergone MR scanning as well as a host of behavioral measures. The scans will be processed with CIVET, cortical thickness maps will be compared in the two groups, and the degree of exposure to

maternal smoking will be regressed against cortical thickness maps.

3.3.5 Corticometric Studies of Developmental Pathology

3.3.5.1 Cross-Sectional Comparison of Patients with Schizophrenia and Normal Controls This component of the thesis project has been completed. and a manuscript will be submitted for publication[153]. The following is a summary of this work.

Subjects and Methods: The subjects of this study have been described in previous reports[2, 3]. 159 patients (112 men, 47 women, mean age: 35.6 yr, SD 12.4) with schizophrenia or schizophreniform disorder and 158 healthy subjects (106 men, 52 women, mean age: 37.7 yr, SD 14.0) from the Utrecht Schizophrenia Project, Utrecht, the Netherlands, participated in this study. Subjects were matched for age, sex, height and socioeconomic status of their parents. An age/illness-duration/illness-severity matching algorithm was followed and there was no statistically significant correlation between severity of illness and age (r=0.01, P=0.88). T1 weighted images were processed in our lab with CIVET, both native (figure 5) and standardized (figre 6) thickness was computed, and each subject's cortical thickness map was blurred using a 20 millimeter full-width half maximum (FWHM) Gaussian smoothing kernel. Statistical analysis was then performed at every vertex without predicting direction of change, regressing cortical thickness against group. To account for multiple comparisons, the resulting statistical maps were set to a specific threshold using the False Discovery Rate (FDR) procedure at a q value of 0.01, the critical t value was calculated as 2.4818. The interpretation of the maps is therefore that 1% of the results shown are, on average, false positives.

Results: Figure 5 is a visual representation of the results. Significant bilateral cortical thinning was present in the lateral prefrontal cortex, the orbitofrontal cortex, the anterior cingulate gyrus, the poles of the temporal lobes and the superior temporal gyrus, and the visual association cortex, in schizophrenic subjects. In addition, the cortex of the right middle temporal gyrus and the left medial temporal cortex were thinner in schizophrenic subjects.

Conclusions: These findings demonstrate the ability of this unique, fully automated, whole-brain method to detect changes in cortical thickness in schizophrenia. The regional distribution of changes found was consistent with independent histopathological and neuroimaging findings on the distribution of neuropathological alterations in schizophrenia, and with gray matter losses previously reported in the same sample when voxel-based morphometric methods were used[2, 3].

3.3.5.2 Childhood-Onset Schizophrenia vs. Controls: A Longitudinal Study Children and adolescents were recruited by the NIMH for an ongoing study of childhood-onset schizophrenia, and have been described in detail in previous reports[157]. Included were 36 patients with childhood-onset schizophrenia (with onset of psychosis before age 12) and 34 healthy volunteers, age and gender matched, both groups having an age range of 8-24 years. All subjects received MR scans at a mean interval of around 2 years. In the COS group, 19 patients had two, 12 had three, and five had four scans for a total of 94 scans. In the normal control group, 19 subjects had two, 13 had three, and two had four scans, for a total of 85 scans.

These scans will undergo a procedure identical to the one mentioned in 4.3.5.1 above, with the exception that statistical analysis will include growth-curve and multivariate analyses.

A subset of this sample (23 COS subjects and 38 controls) when only the first two scans are considered, have been matched to 19 subjects diagnosed with multidimensionally-impaired disorder (MDI), a semi-psychotic disorder that

Figure 5: **t-Statistical Maps of Cortical Thinning Measured in Native Space: The color ligand corresponds to the value of the tstatistic at each vertex. Gray areas have t-stat values below the threshold (q=0.01).** **(a) Front view tilted to the left to expose the left anterior cingulate gyrus (ACG); (b) front view; (c) frontiew tilted to the right to expose the right ACG; (d) right sided view; (e) left sided view; (f) bottom view; (g) top view. [These views are generated by the use of Brain-View software, courtesy of Jason Lerch]**

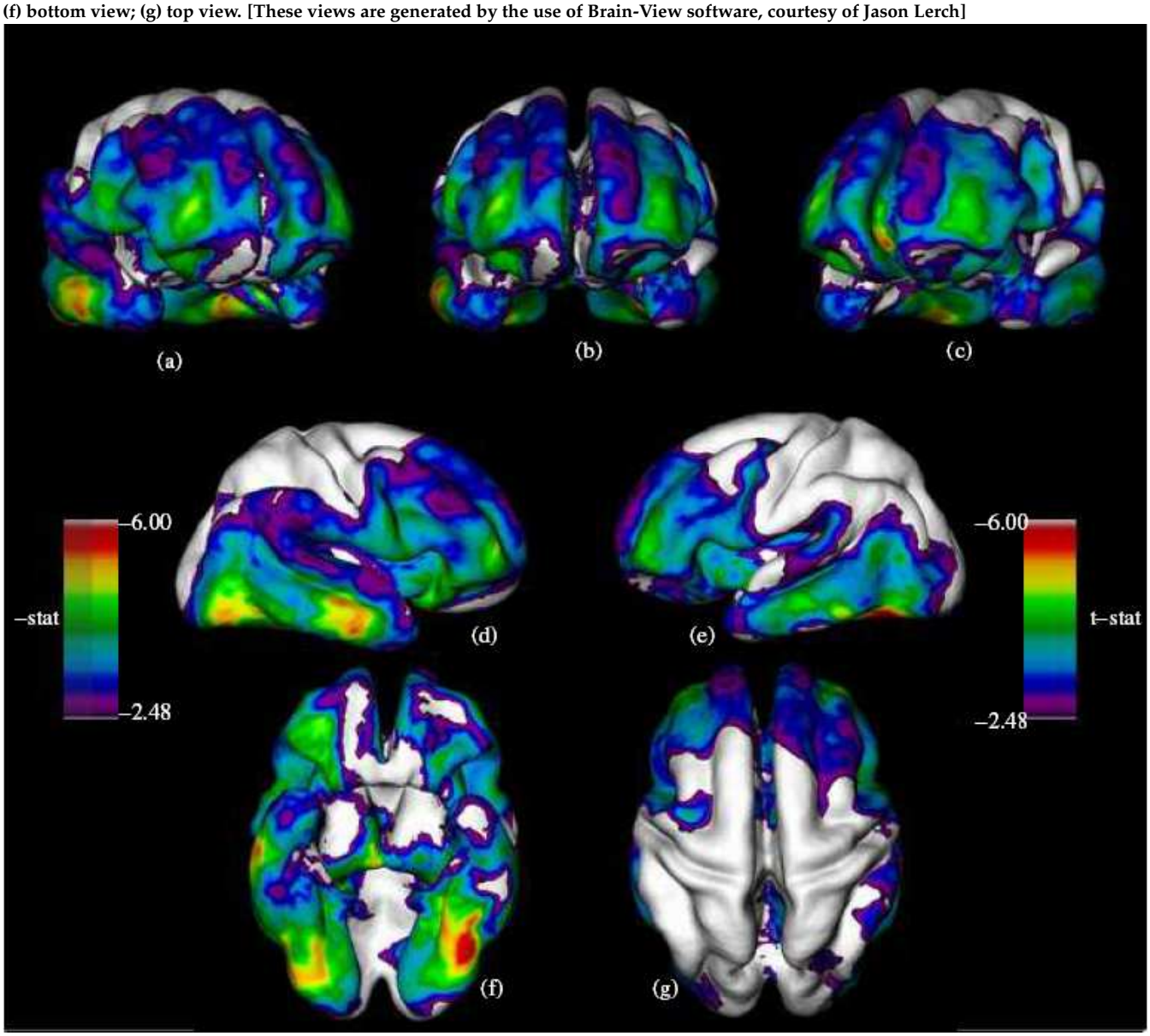

Figure 6: **t-Statistical Maps of Cortical Thinning Measured in Standardized Space: The color ligand corresponds to the value of the tstatistic at each vertex. Gray areas have t-stat values below the threshold (q=0.01). (a) Front view tilted to the left to expose the left anterior cingulate gyrus (ACG); (b) front view; (c) frontiew tilted to the right to expose the right ACG; (d) right sided view; (e) left sided view; (f) bottom view; (g) top view. [These views are generated by the use of Brain-View software, courtesy of Jason Lerch]**

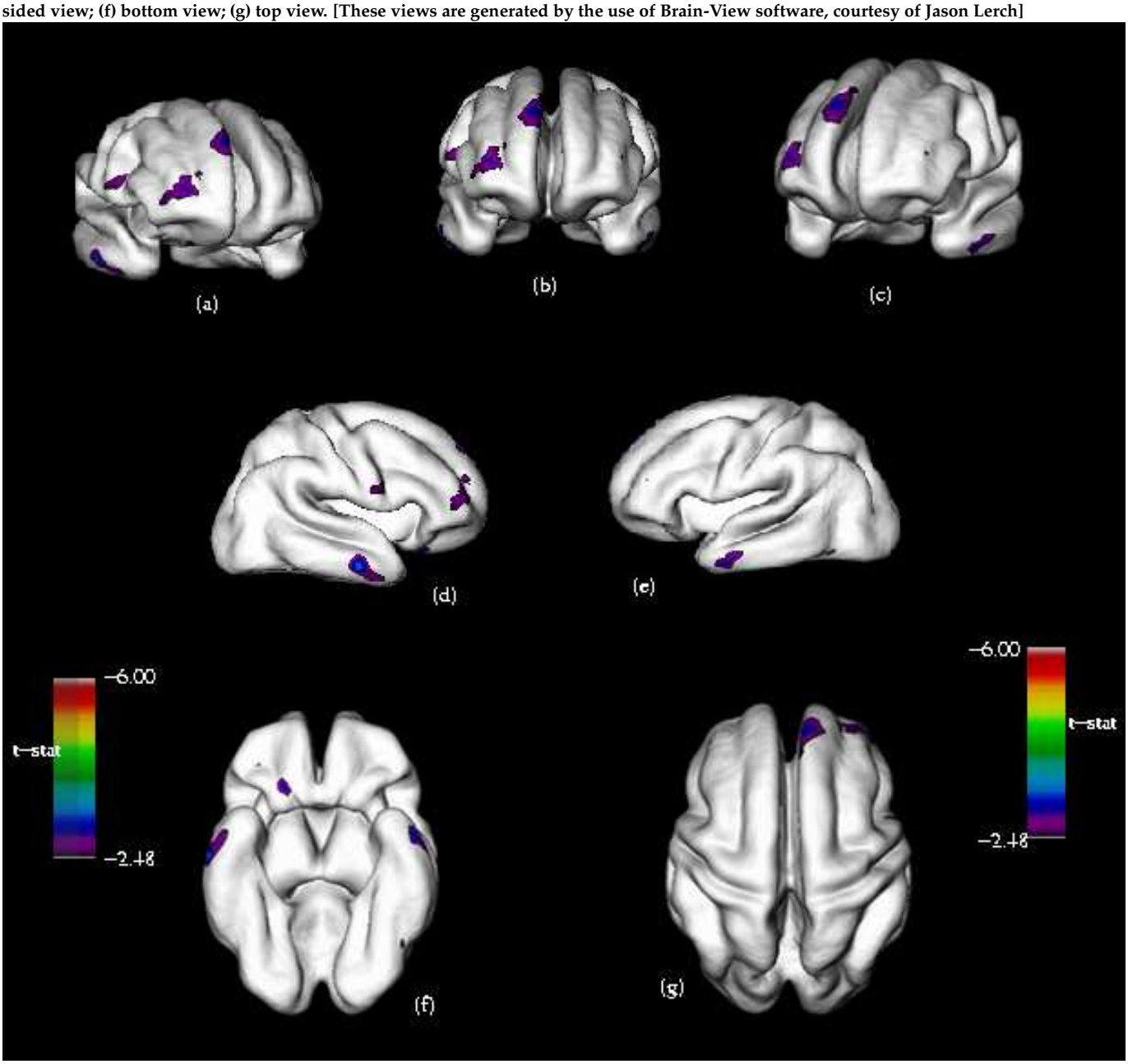

has been described in previous reports[158]. Each of the MDI subjects have also been scanned twice at a mean interval of 2 years. Comparing vertex-based cortical thickness change over time in the 3 groups will provide insight into the specificity of schizophrenia related findings.

3.3.5.3 First-Episode Schizophrenia vs. Controls: A Longitudinal Study The subjects for this study have been described in a previous report[159]. Patients with first-episode schizophrenia (n = 34), recruited from the First-Episode Schizophrenia Research Program at the University Medical Center Utrecht, Utrecht, the Netherlands, and healthy comparison subjects (n = 36) were included in the study. MRI scans of the whole brain were obtained at inclusion (T0) and after 1 year (T1). At inclusion, patients were assessed with the Comprehensive Assessment of Symptoms and History (CASH)[160] by 2 trained raters who independently determined the diagnosis and achieved consensus afterward. The onset of prodromal symptoms and the duration of untreated psychosis were measured by a shortened version of the Interview for the Retrospective Assessment of the Onset of Schizophrenia[161]. Severity of illness was measured with the Positive and Negative Syndrome Scale (PANSS)[162]. Of the 34 patients, 24 had never received anti-psychotic medication. The remaining 10 patients had been prescribed anti-psychotics for less than 16 weeks before the first scan (T0).

At T1, all 34 patients were reassessed for diagnosis and severity of illness using the CASH and the PANSS. The number of days spent in the hospital between T0 and T1 was recorded and used as a measure of 1-year outcome. In addition, every patient was monitored carefully for the amount and type of medication prescribed between T0 and T1. Healthy comparison subjects were carefully matched for sex, age, parental education, and handedness.

The MRI data on this sample was recently received at our lab, and corticometric studies will be performed in a manner similar to the above mentioned experiments. An additional task in the statistical analysis will be the correlation of cortical thickness change over time to changes in the clinical manifestations of schizophrenia.

3.4 Scientific and Clinical Relevance

The emerging ability to study the cerebral neocortex *in vivo* is promising to accelerate the scientific understanding of the developmental processes that determine cortical morphology and function. Although not presently capable of providing exact cytoarchitechtonic information from scans of live humans, the capability will soon be available. Not withstanding the lack of microscopic detail, we now have a method that allows for macroscopic examination of the cerebral cortex during development.

The objective of developing normative growth-curves is not only pioneering, but will likely make available to the scientific community data that can be compared with abnormal developmental trajectories of all causes. This project will also attempt to demonstrate the impact on neocortical development of environmental injury at critical developmental phases, and of severe developmental psychopathology.

In addition, the project is likely to present longitudinal patterns of cortical change that is specific to schizophrenia. Although many neural correlates for schizophrenia exist, specific descriptions of cortical change may allow a targeted approach to histopathological studies of schizophrenia. This in turn may contribute to developing better animal models for the disease, leading to a much greater understanding of the molecular underpinning of schizophrenia. Similar work will be possible with many other neuropsychiatric disorders. There is tremendous value and rich scientific potential in elucidating anatomical correlates of disorders that to date can only be identified via clinical manifestations that are mostly subjective nature. Disorders such autism, ADHD, Tourette's syndrome and childhood depression are but a few examples.

Given the *in vivo* demonstration of both development and plasticity, the longitudinal components of this project will probably set the stage for future experiments that monitor the impact of therapeutic interventions on neocortical anatomy, and develop anatomical correlates of treatment response.

4 Conclusions

This PhD thesis proposal hopes to integrate basic neuroscientific knowledge, neuroimaging and computational technologies, and clinical psychiatric experience in order to increase the breadth of our understanding of the human brain. It is hoped that the proposed research will be a significant scientific contribution to the field of neuroscience. The outlined experiments are heavily computation-dependent, and the capabilities for such work exist at the MNI, and in very few other centers in the world. Since most of the data have been collected, the time required for me to complete the thesis is determined by the image-processing technology, and is likely to be a duration of 2-3 years. Numerous publications in peer-reviewed journals and national and international presentations will result from this work.

References

[1] Kim JC, Singh V, Lerch J, Ad-Dab'bagh Y, MacDonald D, Lee JM, Kim SI, Evans AC. Automated 3-D extraction and evaluation of the outer cortical surface using a Laplacian map and partial volume effect classification. Submitted to NeuroImage, Oct 2003.

[2] Hulshoff Pol HE, Schnack HG, Mandl RC, van Haren NE, Koning H, Collins DL, Evans AC, Kahn RS. Focal gray matter density changes in schizophrenia. Arch Gen Psychiatry. 2001; 58:1118-1125.

[3] Hulshoff Pol HE, Schnack HG, Bertens MG, van Haren NE, van der Tweel I, Staal WG, Baare WF, Kahn RS. Volume changes in gray matter in patients with schizophrenia. Am J Psychiatry. 2002; 159:244-250.

[4] Genari 1776. In Perceptual Neuroscience: The Cerebral Cortex (Mountcastle VB, Ed., 1998), Harvard Univ. Press, Cambridge, MA.

[5] Betz 1874. In The Cytoarchitectonics of the Human Cerebral Cortex (Von Economo, Ed., 1929), translated by S. Parker. Oxford Univ. Press, Oxford.

[6] Meynert 1867. In The Cytoarchitectonics of the Human Cerebral Cortex (Von Economo, Ed., 1929), translated by S. Parker. Oxford Univ. Press, Oxford.

[7] Brodmann K. 1905. In Perceptual Neuroscience: The Cerebral Cortex (Mountcastle VB, Ed., 1998), Harvard Univ. Press, Cambridge, MA.

[8] Brodmann K. Vergleichende Lokalisationslehre der Grosshirnrinde in ihren Prinzipen dargestellt auf Grund des Zellenbaues. Barth, Leipzig, 1909.

[9] Brodmann K. 1914. In Perceptual Neuroscience: The Cerebral Cortex (Mountcastle VB, Ed., 1998), Harvard Univ. Press, Cambridge, MA.

[10] Vogt O, Vogt C. 1919. In Perceptual Neuroscience: The Cerebral Cortex (Mountcastle VB, Ed., 1998), Harvard Univ. Press, Cambridge, MA.

[11] von Economo C. 1929. The Cytoarchitectonics of the Human Cerebral Cortex. Translated by S. Parker. Oxford Univ. Press, Oxford.

[12] Sarkisov S, Filimonoff I, Kononowa E, Preobraschenskaja I, Kukuew L. 1955. Atlas of the Cytoarchitectonics of the Human Cerebral Cortex. Medgiz, Moscow.

[13] Haug H, Kuhl S, Mecke E, Sass N, Wasner K. The significance of morphometric procedures in the investigation of age changes in cytoarchitectonic structures of the human brain. Int. J. Brain Res. Neurobiol. 1984; 25:353-374.

[14] Rajkowska G, Goldman-Rakic P. Cytoarchitectonic definition of prefrontal areas in the normal human cortex: I. Remapping of areas 9 and 46 using quantitative criteria. Cerebral Cortex 1995; 5:307-322.

[15] Rajkowska G, Goldman-Rakic P. Cytoarchitectural definition of prefrontal areas in the normal human cortex: II. Variability in locations of area 9 and 46 and relationship to the Talairach coordinate system. Cerebral Cortex 1995; 5:323-338.

[16] Ameral DG. The Anatomical Organization of the Central Nervous System. In Eric R. Kandel, James H. Schwartz, and Thomas M. Jessel, editors, Principles of Neural Science. McGraw Hill, fourth edition, 2000.

[17] Kabani N, Le Goualher G, MacDonald D, Evans AC. Measurement of cortical thickness using an automated 3-D algorithm: A validation study. NeuroImage 2001; 13:375-380.

[18] Mountcastle VB. 1998. Perceptual Neuroscience: The Cerebral Cortex. Harvard Univ. Press, Cambridge, MA.

[19] Snell RS. Clinical Neuroanatomy for Medical Students; 2nd edition. Little, Brown and Company, Inc. Toronto, 1987.

[20] Obermayer K, Blasdel GG. Geometry of orientation and occular dominance columns in monkey striate cortex. J Neurosci 1993; 13:4115-4129.

[21] Krubitzer L, Kahn DM. Nature versus nurture revisited: an old idea with a new twist. Prog Neurobiol 2003; 70:33-52.

[22] McConnell SK. Strategies for the generation of neuronal diversity in the developing central nervous system. J Neurosci 1995; 15:6987-98.

[23] Levitt P. Development of the vetebrate nervous system. In: Wong-Riley MTT, editor. Neuroscience secrets. Volume 3. Philadelphia: Hanley & Belfus, Inc; 1999. p. 46-57.

[24] Levitt P. Structural and functional maturation of the developing primate brain. J Pediatr 2003; 143:S35-S45

[25] Sidman RL, Rakic P. Neuronal migration with special reference to the human brain: a review. Brain Res 1973; 62:1-35.

[26] Monk CS, Webb SJ, Nelson CA. Prenatal neurobiological development: molecular mechanisms and anatomical changes. Dev Neuropsychol 2001; 19:211-236.

[27] Webb SJ, Monk CS, Nelson CA. Mechanisms of postnatal neurobiological development: implications for human development. Dev Neuropsychol 2001; 19:147-171.

[28] Kostović I. Structural and histochemical reorganization of the human prefrontal cortex during perinatal and postnatal life. Prog Brain Res 1990; 85:223-240.

[29] Kostović I. Rakic P. Developmental history of the transient subplate zone in the visual and somatosensory cortex of the macaque monkey and human brain. J Comp Neurol 1990; 297:441-470.

[30] Rakic P. A small step for the cell, a giant leap for mankind: a hypothesis of neocortical expansion during evolution. Trends Neurosci 1995; 18:383-388.

[31] Ulfig N, Neudorfer F, Bohl J. Transient structures of the human fetal brain: subplate, thalamic reticular complex, ganglionic eminence. Histol Histopathol 2000; 15:771-790.

[32] Rice D, Barone S Jr. Critical periods of vulnerability for the developing nervous system: evidence from humans and animal models. Environ Health Perspect 2000; 108 Suppl 3:511-533.

[33] Kornack DR. Neurogenesis and the evolution of cortical diversity: mode, tempo, and partitioning during development and persistence in adulthood. Brain Behav Evol 2000; 55:336-344.

[34] Bourgeois JP. Synaptogenesis, heterochrony and epigenesis in the mammalian cerebral cortex. Acta Paediatr Suppl 1997; 422:27-33.

[35] Molliver ME, Kostović I, van der Loos H. The development of synapses in cerebral cortex of the human fetus. Brain Res 1973; 50:403-407.

[36] Pencea V, Bingaman KD, Freedman LJ, Luskin MB. Neurogenesis in the subventricular zone and rostral migratory stream of the neonatal and adult primate forebrain. Exp Neurol 2001; 172:1-16.

[37] Eriksson PS, Perfilieva E, Bjork-Eriksson T, Alborn AM, Nordborg C, Peterson DA, et al. Neurogenesis in the adult human hippocampus. Nat Med 1998; 4:1313-1317.

[38] Kornack DR, Rakic P. Cell proliferation without neurogenesis in adult primate neocortex. Science 2001; 294:2127-2130.

[39] Olson L, Boreus IO, Seiger A. Histochemical demonstration and mapping of 5-hydroxytrypamine- and catecholamine-containing neuron systems in the human fetal brain. Z Anat Entwickl-Gesch 1973; 139:259-282.

[40] Nobin A, Bjorklund A. Topography of the monoamine neuron system in the human brain as revealed in fetuses. Acta Physiol Scand 1973; 388:1-40.

[41] Mrzljak L, Uylings HBM, Van Eden CG, Judas M. Neuronal development in human prefrontal cortex in prenatal and postnatal stages. Prog Brain Res 1990; 85:185-222.

[42] Kostović I, Judas M, Petanjek Z, Simic G. Ontogenesis of goal-directed behavior: anatomo-functional considerations. Int J Psychophysiol 1995; 19:85-102.

[43] Rakic P, Bourgeois JP, Eckenhoff MF, Zecevic N, Goldman-Rakic PS. Concurrent overproduction of synapses in diverse regions of the primate cerebral cortex. Science 1986; 232:232-235.

[44] Huttenlocher PR, Dabholkar AS. Regional differences in synaptogenesis in human cerebral cortex. J Comp Neurol 1997; 387:167-178.

[45] Innocenti, G.M. Development of interhemispheric cortical connections. Neurosci Res Prog Bull 1982; 20:532-540.

[46] Pollak SD, Kistler DJ. Early experience is associated with the development of categorical representations for facial expressions of emotion. Proc Natl Acad Sci U S A 2002; 99:9072-9076.

[47] Paus T, Collins DL, Evans AC, Pike LB, Zijdenbos A. Maturation of white matter in the human brain: a review of magnetic resonance studies. Brain Res Bull 2001; 54:255-266.

[48] Courchesne E. Abnormal early brain development in autism. Mol Psychiatry 2002; 7 Suppl 2:S21-S23.

[49] Carper RA, Moses P, Tigue ZD, Courchesne E. Cerebral lobes in autism: early hyperplasia and abnormal age effects. Neuroimage 2002; 16:1038-1051.

[50] Landing BH, Shankle WR, Hara J, Brannock J, Fallon JH. The development of structure and function in the postnatal human cerebral cortex from birth to 72 months: changes in thickness of layers II and III co-relate to the onset of new age-specific behaviors. Pediatr Pathol Mol Med 2002; 21:321-342.

[51] Huttenlocher, P.R. Synaptic density in human frontal cortex: Developmental changes and effects of aging. Brain Res 1979; 163:195-205.

[52] Benes FM, Turtle M, Khan Y, Farol P. Myelination of a key relay zone in the hippocampal formation occurs in the human brain during childhood, adolescence, and adulthood. Arch Gen Psychiatry 1994; 51:477-484

[53] Sowell ER, Thompson PM, Tessner KD, Toga AW. Mapping continued brain growth and gray matter density reduction in dorsal frontal cortex: Inverse relationships during postadolescent brain maturation. J Neurosci 2001; 21:8819-8829.

[54] Braak H, Braak E. Staging of Alzheimer's Disease-Related Neurofibrillary Changes. Neurobiology of Aging 1995; 16:271-284.

[55] Buldyrev SV, Cruz L, Gomez-Isla T, Gomez-Tortosa E, Havlin S, Le R, Stanley HE, Urbanc B, Hyman BT. Description of microcolumnar ensembles in association cortex and their disruption in Alzheimer and lewy body dementias. PNAS 2000; 97:5039-5043.

[56] Salat DH, Kaye JA, Janowsky JS. Selective preservation and degeneration within the prefrontal cortex in aging and Alzheimer disease. Arch Neurol 2001; 58:1403-1408.

[57] Mann DMA, Oliver R, Snowden JS. The topographic distribution of brain atrophy in Huntington's disease and progressive supranuclear palsy. Acta Neuropathol 1993; 85: 553-559.

[58] Kemper TL, Bauman ML. Neuropathology of infantile autism. Mol Psychiatry 2002; 7 Suppl 2:S12-S13.

[59] Bailey A, Luthert P, Dean A, Harding B, Janota I, Montgomery M, Rutter M, Lantos P. A clinicopathological study of autism. Brain 1998; 121:889-905.

[60] Kanner L. Follow-up study of eleven autistic children originally reported in 1943: 1971. Psychiatr Enfant 1995; 38:421-461.

[61] Tenkova T, Young C, Dikranian K, Labruyere J, Olney JW. Ethanol-induced apoptosis in the developing visual system during synaptogenesis. Invest Ophthalmol Vis Sci 2003; 44:2809-2817.

[62] Granato A, Van Pelt J. Effects of early ethanol exposure on dendrite growth of cortical pyramidal neurons: inferences from a computational model. Brain Res Dev Brain Res 2003; 142:223-227.

[63] Wass TS, Persutte WH, Hobbins JC. The impact of prenatal alcohol exposure on frontal cortex development in utero. Am J Obstet Gynecol 2001; 185:737-742.

[64] Konovalov HV, Kovetsky NS, Bobryshev YV, Ashwell KW. Disorders of brain development in the progeny of mothers who used alcohol during pregnancy. Early Hum Dev 1997; 48:153-166.

[65] Benes FM, Davidson J, Bird ED. Quantitative cytoarchitectural studies of the cerebral cortex of schizophrenics. Arch Gen Psychiatry 1986; 43:31-35.

[66] Benes FM, Bird ED. An analysis of the arrangement of neurons in the cingulate cortex of schizophrenic patients. Arch Gen Psychiatry 1987; 44:608-616.

[67] Bouras C, Kovari E, Hof PR, Riederer BM, Giannakopoulos P. Anterior cingulate cortex pathology in schizophrenia and bipolar disorder. Acta Neuropathol (Berl) 2001; 102:373-379.

[68] Kawasak Y, Vogeley K, Jung V, Tepest R, Hutte H, Schleicher A, Falkai P. Automated image analysis of disturbed cytoarchitecture in Brodmann area 10 in schizophrenia: a post-mortem study. Prog Neuropsychopharmacol Biol Psychiatry 2000; 24:1093-1104.

[69] Arnold SE, Trojanowski JQ. Recent advances in defining the neuropathology of schizophrenia. Acta Neuropathol (Berl) 1996; 92:217-231.

[70] Pakkenberg B. Total nerve cell number in neocortex in chronic schizophrenic and controls estimated using optical disectors. Biol Psychiatry 1993; 34:768-772.

[71] Heckers S. Neuropathology of schizophrenia: cortex, thalamus, basal ganglia, and neurotransmitter-specific projection systems. Schizophr Bull 1997; 23:403-421.

[72] Pierri JN, Volk CLE, Auh S, Sampson A, Lewis DA. Decreased somal size of deep layer 3 pyramidal neurons in the prefrontal cortex of subjects with schizophrenia. Arch Gen Psychiatry 2001; 58:466-473.

[73] Rajkowska G, Selemon LD, Goldman-Rakic PS. Neuronal and glial somal size in the prefrontal cortex: A postmortem morphometric study of schizophrenia and Huntington disease. Arch Gen Psychiatry 1998; 55:215-224.

[74] Garey LJ, Ong WY, Patel TS, Kanani M, Davis A, Mortimer AM, Barnes TRE, Hirsch SR. Reduced dendritic spine density on cerebral cortical pyramidal neurons in schizophrenia. J Neurol Neurosurg Psychiatry 1998; 65:446-453.

[75] Glantz LA, Lewis DA. Decreased dendritic spine density on prefrontal cortical pyramidal neurons in schizophrenia. Arch Gen Psychiatry 2000; 57:65-73.

[76] Chana G, Landau S, Beasley C, Everall IP, Cotter D. Two-dimensional assessment of cytoarchitecture in the anterior cingulate cortex in major depressive disorder, bipolar disorder, and schizophrenia: evidence for decreased neuronal somal size and increased neuronal density. Biol Psychiatry 2003; 53:1086-1098.

[77] Benes FM, Sorensen I, Bird ED. Reduced neuronal size in posterior hippocampus of schizophrenic patients. Schizophr Bull 1991; 17:597-608.

[78] Browning MD, Dudek EM, Rapier JL, Leonard S, Freedman R. Significant reductions in synapsin but not synaptophysin specific activity in the brains of some schizophrenics. Biol Psychiatry 1993; 34:529-535.

[79] Kovelman JA, Scheibel AB. A neurohistological correlate of schizophrenia. Biol Psychiatry 1984; 19:1601-1621.

[80] Conrad AJ, Abebe T, Austin R, Forsythe S, Scheibel AB. Hippocampal pyramidal cell disarray in schizophrenia as a bilateral phenomenon. Arch Gen Psychiatry 1991; 48:413-417.

[81] Curtis VA, van Os J, Murray RM. The Kraepelinian dichotomy: evidence from developmental and neuroimaging studies. J Neuropsychiatry Clin Neurosci 2000; 12:398-405.

[82] Verdoux H. International collaborative study of the association between schizophrenia and obstetric complications. Relationships between obstetric complications, age of onset, gender and family history. Eur Psychiatry 1996; 11 (Suppl 4):211.

[83] Jones P, Rodgers B, Murry R, Marmot M. Child development risk factors for adult schizophrenia in the British 1946 birth cohort. The Lancet 1994; 344:1398-1402.

[84] Done D, Crow TJ, Johnstone EC, Sacker A. Childhood antecedents of schizophrania and affective illness: social adjustment at ages 7 and 11. Br Med J 1994; 309:699-703.

[85] Jones P, Rantakallio P, Hartikainen A-L, Isohanni M, Sipila. P. Does schizophrenia result from pregnancy, delivery and perinatal complications? A 28 year study in the 1966 North Finland birth cohort. Eur Psychiatry 1996; 11 (Suppl 4):242.

[86] Bracha HS (1991). Etiology of structural asymmetry in schizophrenia: an alternative hypothesis. Schizophr Bull 1991; 17: 551-553.

[87] Davis JO, Bracha HS. Prenatal growth markers in schizophrenia: a monozygotic co-twin control study. Am J Psychiatry 1996; 153:1166-1172.

[88] Rosa A, Fananas L, Bracha HS, Torrey EF, van Os J. Am J Psychiatry 2000; 157:1511-1513.

[89] Bayer TA, Falkai P, Maier W. Genetic and non-genetic vulnerability factors in schizophrenia: the basis of the "two-hit hypothesis". J Psychiatr Res 1999; 33:543-548.

[90] Maynard TM, Sikich L, Lieberman JA, LaMantia AS. Neural development, cell-cell signaling, and the "two-hit" hypothesis of schizophrenia. Schizophr Bull 2001; 27:457-476.

[91] Schleicher A, Amunts K, Geyer S, Morosan P, Zilles K. Observer-independent method for microstructural parcellation of cerebral cortex: A quantitative approach to cytoarchitectonics. Neuroimage 1999; 9:165-177.

[92] Hinton VJ. Ethics of neuroimaging in pediatric development. Brain Cogn 2002; 50:455-468.

[93] Eliez S, Reiss AL. MRI neuroimaging of childhood psychiatric disorders: a selective review. J Child Psychol Psychiatry 2000; 41:679-694.

[94] Giedd JN, Snell JW, Lange N, Rajapakse JC, Casey BJ, Kozuch PL, Viatuzis AC, Vauss YC, Hamburger SD, Kaysen D, Rapoport JL. Quantitative magnetic resonance imaging of human brain development: ages 4-18. Cerebral Cortex 1996; 6:551-560.

[95] Giedd JN, Vaituzis AC, Hamburger SD, Lange N, Rajapakse JC, Kaysen D, Vauss YC, Rapoport JL. Quantitative MRI of the temporal lobe, amygdala, and hippocampus in normal human development: ages 4-18 years. J Compar Neurol 1996; 366:223-230.

[96] Reiss AL, Abrams MT, Singer HS, Ross JL, Denckla MB. Brain development, gender and IQ in children. a volumetric imaging study. Brain 1996; 119:1763-1774.

[97] Giedd JN, Blumenthal J, Jeffries NO, Castellanos FX, Lui H, Zijdenbos A, Paus T, Evans AC, Rapoport JL. Brain Development during childhood and adolescence: a longitudinal MRI study. Nat Neurosci 1999; 2:861-863.

[98] Pfefferbaum A, Mathalon DH, Sullivan EV, Rawles JM, Zipursky RB, Lim KO. A quantitative magnetic resonance imaging study of changes in brain morphology from infancy to late adulthood. Arch Neurol 1994; 51:874-887.

[99] Caviness VS, Kennedy DN, Richelme C, Rademacher J, Filipek PA. The human brain age 7-11 years: a volumetric analysis based on magnetic resonance images. Cereb Cortex 1996; 6:726-736.

[100] Paus T, Zijdenbos A, Worsley K, Collins DL, Blumenthal J, Giedd JN, Rapoport JL, Evans AC. Structural maturation of neural pathways in children and adolescents: in vivo study. Science 1999; 283:1908-1911.

[101] Matsuzawa J, Matsui M, Konishi T, Noguchi K, Gur RC, Bilker W, Miyawaki T. Age-related volumetric changes of brain gray and white matter in healthy infants and children. Cereb Cortex 2001; 11:335-342.

[102] Ballesteros MC, Hansen PE, Soila K. MR imaging of the developing human brain. Part 2. Postnatal development. Radiographics 1993; 13:611-622.

[103] Talairach J, Tournoux P. Coplanar stereotaxic atlas of the human brain. Thieme Medical, New York, 1988.

[104] Collins DL, Neelin P, Peters TM, Evans AC. Automatic 3D intersubject registration of MR volumetric data in standardized Talairach space. J Comput Assist Tomogr 1994; 18:192-205.

[105] Shattuck DW, Sandor-Leahy SR, Schaper KA, Rottenberg DA, Leahy RM. Magnetic resonance image tissue classification using a partial volume model. Neuroimage 2001; 13:856-876.

[106] Autti T, Raininko R, Vanhanen SL, Kallio M, Santavuori P. MRI of the normal brain from early childhood to middle age. II. Age dependence of signal intensity changes on T2-weighted images. Neuroradiology 1994; 36:649-651.

[107] von Economo C, Koskinas GN. Die Cytoarchitektonik der Hinrinde des erwachsenen Menschen. Julius Springer Inc. Berlin 1925.

[108] Meyer JR, Roychowdhury S, Russell EJ, Callahan C, Gitelman D, Mesulam MM. Location of the central sulcus via cortical thickness of the precentral and postcentral gyri on MR. Am J Neuroradiol 1996; 17:1699-1706.

[109] MacDonald D, Kabani N, Avis D, Evans AC. Automated 3-D extraction of inner and outer surfaces of cerebral cortex from MRI. NeuroImage 2000; 12:340-356.

[110] Lorensen WE, Cline HE. Marching cubes: A high resolution 3-d surface construction algorithm. Comput Graph Quart Rep SIGGRAPH-ACM 1987; 21:163-169.

[111] McInerney T, Terzopoulos D. Deformable models in medical image analysis: a survey. Med Image Anal 1996; 1:91-108.

[112] Dale AM, Fischl B, Sereno MI. Cortical surface-based analysis. I. Segmentation and surface reconstruction. Neuroimage 1999; 9:179-194.

[113] Fischl B, Sereno MI, Dale AM. Cortical surface-based analysis. II: Inflation, flattening, and a surface-based coordinate system. Neuroimage 1999; 9:195-207.

[114] Fischl B, Dale AM. Measuring the thickness of the human cerebral cortex from magnetic resonance images. Proc Natl Acad Sci U S A. 2000 Sep 26;97(20):11050-5.

[115] Rosas HD, Liu AK, Hersch S, Glessner M, Ferrante RJ, Salat DH, van der Kouwe A, Jenkins BG, Dale AM, Fischl B. Regional and progressive thinning of the cortical ribbon in Huntington's disease. Neurology 2002 58:695-701, 2002.

[116] Kuperberg GR, Broome MR, McGuire PK, David AS, Eddy M, Ozawa F, Goff D, West WC, Williams SC, van der Kouwe AJ, Salat DH, Dale AM, Fischl B. Regionally localized thinning of the cerebral cortex in schizophrenia. Arch Gen Psychiatry 2003; 60:878-888.

[117] Sailer M, Fischl B, Salat D, Tempelmann C, Schonfeld MA, Busa E, Bodammer N, Heinze HJ, Dale A. Focal thinning of the cerebral cortex in multiple sclerosis. Brain 2003; 126:1734-1744.

[118] Han X, Xu C, Braga-Neto U, Prince JL. Topology correction in brain cortex segmentation using a multiscale, graph-based algorithm. IEEE Trans Med Imaging 2002; 21:109-121.

[119] Kriegeskorte N, Goebel R. An efficient algorithm for topologically correct segmentation of the cortical sheet in anatomical MR volumes. Neuroimage 2001; 14:329-346.

[120] Zeng X, Staib LH, Schultz RT, Duncan JS. Segmentation and measurement of the cortex from 3-D MR images using coupled-surfaces propagation. IEEE Trans Med Imaging 1999; 18:927-937.

[121] Lerch J, Pruessner J, Zijdenbos A, Evans AC. A validation study of cortical thickness analysis. Proceedings of the 9th Annual Meeting of the Organization for Human Brain Mapping. 2003.

[122] References Lerch J, Zijdenbos A., Goto R, Taki Y, Sato K, Kawashima R, Fukuda H, Evans AC. Cortical thinning in aging. Proceedings of the 9th Annual Meeting of the Organization for Human Brain Mapping. 2003.

[123] Lerch J, Pruessner J, Zijdenbos, Teipel SJ, Buerger K, Hampel H, Evans AC. Changes in cortical Integrity in alzheimer's disease. Proceedings Conference on Alzheimer's Disease and Related Disorders. 2002.

[124] Lerch J, Bernasconi N, Bernasconi A, Evans AC. Cortical thickness in left temporal lobe epilepsy. Proceedings of the 9th Annual Meeting of the Organization for Human Brain Mapping. 2003.

[125] Tohka J, Zijdenbos A, Evans A. Fast and robust parameter estimation for statistical partial volume models in brain MRI. 2003 (Submitted).

[126] Ma CM, Wan SY, Lee JD. Three-dimensional topology preserving reduction on the 4-subfields. IEEE Transactions on Pattern Analysis and Machine Intelligence 2002; 24:1594-1605.

[127] Jones SE, Buchbinder BR, Aharon I. Three-dimensional mapping of cortical thickness using Laplace's equation. Hum Brain Mapp 2000; 11:12-32.

[128] Friston KJ, Holmes AP, Worsley KJ. How many subjects constitute a study? Neuroimage 1999; 10:1-5.

[129] Nieto-Castanon A, Ghosh SS, Tourville JA, Guenther FH. Region of interest based analysis of functional imaging data. Neuroimage 2003; 19:1303-1316.

[130] Shaffer, JP. Multiple hypothesis testing. Annu Rev Psychol 1995; 46:561-584.

[131] Petersson KM, Nichols TE, Poline JP, Holmes AP. Statistical limitations in functional neuroimaging II. Signal detection and statistical inference. Phil Trans R Soc Lond B 1999; 354:1261-1281.

[132] Worsley KJ, Marrett S, Neelin P, Evans AC. A unified statistical approach for determining significant signals in location and scale space images of cerebral activation. In: Myers R, Cunningham VJ, Bailey DL, Jones T, eds. Quantification of brain function using PET. Academic Press, San Diego 1995; 327-333.

[133] Worsley KJ, Marrett S, Neelin P, Vandal S, Friston KJ, Evans AC. A unified statistical approach for determining significant signals in images of cerebral activation. Hum Brain Mapp 1996; 4:58-73.

[134] Worsley KJ. The geometry of random images. Chance 1996; 9:27-40.

[135] Worsley KJ, MacDonald D, Cao J, Shafie Kh, Evans AC. Statistical analysis of cortical surfaces. NeuroImage 1996; 3:S108.

[136] Worsley KJ. An overview and some new developments in the statistical analysis of PET and fMRI data. Human Brain Mapping 1997; 5:254-258.

[137] Chung MK, Worsley KJ, Paus T, Robbins S, Taylor J, Giedd JN, Rapoport JL, Evans AC. Tensor-based surface morphometry. Technical Report 1049, Department of Statistics, University of Wisconsin. Madison 2002.

[138] Holmes AP, Blair RC, Watson JD, Ford I. Nonparametric analysis of statistic images from functional mapping experiments. Cereb Blood Flow Metab 1996; 16:7-22.

[139] Nichols TE, Holmes AP. Nonparametric permutation tests for functional neuroimaging: a primer with examples. Hum Brain Mapp 2002; 15:1-25.

[140] Benjamini Y, Hochberg Y. Controlling the false discovery rate: a practical and powerful approach to multiple testing. J R Stat Soc Ser B 1995; 57:289-300.

[141] Genovese CR, Lazar NA, Nichols T. Thresholding of statistical maps in functional neuroimaging using the false discovery rate. Neuroimage 2002; 15:870-878.

[142] Zijdenbos AP, Forghani R, Evans AC. Automatic "pipeline" analysis of 3-D MRI data for clinical trials: application to multiple sclerosis. IEEE Trans Med Imaging 2002; 21:1280-1291.

[143] Sled JG, Zijdenbos AP, Evans AC. A nonparametric method for automatic correction of intensity nonuniformity in MRI data. IEEE Trans Med Imaging 1998; 17:87-97.

[144] Zijdenbos A, Forghani R, Evans A. Automatic quantification of MS lesions in 3D MRI brain data sets: validation of INSECT. In: Wells WM, Colchester A, Delp S, eds. MICCAI'98, LNCS 1998; 1496:439-448.

[145] Evans AC, Peters TM, Collins DL, Henri CJ, Marrett T, Pike GB, Dai W. 3-D correlative imaging and segmentation of cerebral anatomy, function and angiography. *IEEE Trans Eng Med Biol* 1990; 12:1297-1298.

[146] Evans AC, Marrett S, Torrescorzo J, Ku S, Collins DL. MRI-PET correlation in three dimensions using a volume-of-interest (VOI) atlas. *Journal of Cerebral Blood Flow and Metabolism* 1991; 11: A69-A78.

[147] Evans AC, Collins DL, Mills SR, Brown ED, Kelly L. 3D statistical neuroanatomical models from 305 MRI volumes. *IEEE Proceedings Nuclear Science Symposium and Medical Imaging Conference* 1993; 1813-1817.

[148] Robbins S. Anatomical standardization of the human brain in Euclidean 3-space and on the cortical 2-manifold. Ph.D Thesis, School of Computer Science, McGill University. 2003.

[149] Ad-Dab'bagh Y, Lerch J, Robbins S, Singh V, Kim JC, Fombonne E, Hulshoff Pol HE, Kahn RS, Evans AC. A comparison of cortical thickness measurements in native and standardized spaces: implications for clinical populations. To be submitted to NeuroImage Nov 2003.

[150] MacDonald D. A method for identifying geometrically simple surfaces from three dimensional images. PhD thesis, School of Computer Science, McGill University. 1997.

[151] Ripley BD. The R project in statistical computing. MSOR Connections. The newsletter of the LTSN Maths, Stats & OR Network 2001; 1:23-25.

[152] MATLAB 6.1.0 for Unix. The MathWorks, Natick, MA.

[153] Ad-Dab'bagh Y, Hulshoff Pol HE, Lerch J, Robbins S, Schnack HG, van Haren NEM, Fombonne E, Evans AC, Kahn RS. Case-control comparison of cortical thickness maps in schizophrenia: an anatomical MRI study. To be submitted to the American Journal of Psychiatry, November 2003.

[154] Ashburner J, Friston KJ. Voxel-based morphometry–the methods. *Neuroimage* 2000; 11:805-821.

[155] Statistics Canada. National Longitudinal Study on Children and Youth, 1994-1995 Data. Ottawa, Ontario: Statistics Canada.

[156] The Protocol for the "Pediatric Brain MRI Database and Study of Normal Development". October 2000. URL: http://www.bic.mni.mcgill.ca/nihpd/ . Public URL: http://www.brain-child.org/ .

[157] Keller A, Castellanos FX, Vaituzis AC, Jeffries NO, Giedd JN, Rapoport JL. Progressive loss of cerebellar volume in childhood-onset schizophrenia. *Am J Psychiatry* 2003; 160:128-133.

[158] Kumra S, Jacobsen LK, Lenane M, Zahn TP, Wiggs E, Alaghband-Rad J, Castellanos FX, Frazier JA, McKenna K, Gordon CT, Smith A, Hamburger SD, Rapoport JL. "Multidimensionally impaired disorder": is it a variant of very early-onset schizophrenia? *J Am Acad Child Adolesc Psychiatry* 1998; 37:91-99.

[159] Cahn W, Pol HE, Lems EB, van Haren NE, Schnack HG, van der Linden JA, Schothorst PF, van Engeland H, Kahn RS. Brain volume changes in first-episode schizophrenia: a 1-year follow-up study. *Arch Gen Psychiatry* 2002; 59:1002-1010.

[160] Andreasen NC, Arndt S. The Comprehensive Assessment of Symptoms and History (CASH): an instrument for assessing diagnosis and psychopathology. *Arch Gen Psychiatry* 1992; 49:615-623.

[161] Hãfner H, Riecher-Rössler A, Hambrecht M, Maurer K, Meissner S, Schmidtke A, van der Heiden W. IRAOS: an instrument for the assessment of onset and early course of schizophrenia. *Schizophr Res* 1992; 6:209-223.

[162] Kay SR, Fiszbein A, Opler LA. The Positive and Negative Syndrome Scale (PANSS) for schizophrenia. *Schizophr Bull* 1987; 13:261-276.